Strain echocardiography in cardiac surgery

Studies on the effects of loading conditions and inotropic agents on myocardial contraction and relaxation

Martin Fredholm

Department of Anesthesiology
and Intensive Care,
Institute of Clinical Sciences at
Sahlgrenska Academy
University of Gothenburg

Gothenburg, Sweden, 2019

UNIVERSITY OF
GOTHENBURG

Cover illustration: Strain curve of the left ventricular inferior wall from speckle tracking echocardiography after passive leg elevation.

Strain echocardiography in cardiac surgery –
Studies on the effects of loading conditions and inotropic agents on myocardial contraction and relaxation

martin.fredholm@gu.se
ISBN: 978-91-7833-738-5 (PRINT)
ISBN: 978-91-7833-739-2 (PDF)
http://hdl.handle.net/2077/62215

Printed in Gothenburg, Sweden, November 2019
Printed by BrandFactory

Till Marina, Edit och Sixten

"In questions of science,
the authority of a thousand
is not worth the humble reasoning
of a single individual."
Galileo Galilei

Abstract

Background: Although reductions in myocardial contractility and relaxation are key components in heart failure (HF), assessment of them is difficult, as clinical measurements deal with a net effect of myocardial contractility, heart filling (preload), outflow impedance (afterload) and heart rate (HR). Echocardiographic (echo) deformation parameters, like strain (myocardial shortening) and strain rate (the speed of deformation, SR), have been proposed to more accurately measure myocardial function, but incongruent previous studies have raised concerns that they may be load-dependent. This load-dependency of echo measurements in general also explains the difficulties assessing right ventricular (RV) function whenever left ventricular (LV) failure is present. Lastly, the inodilators milrinone (MIL) and levosimendan (LEV), often used in treating severe HF, have never been compared head-to-head taking this load-dependency into account.

Aims and methods: We wanted to evaluate whether strain and SR were dependent on preload, afterload and HR (paper I). While keeping cardiac loading and HR constant, we compared the myocardial effects of MIL vs. LEV in a randomized trial, combining echo (for strain and systolic (SR-S) and diastolic (SR-E) SR) with hemodynamic measurements from a pulmonary artery catheter (papers II–III). We included post-cardiac surgery aortic stenosis patients with normal LV function for papers I–III. In paper IV, we retrospectively compared echo indices of RV function with right heart catheterization data in patients with severe HF, creating three groups: A) right atrial pressure (RAP) <10 mmHg and stroke volume index (SVI) ≥35 ml/m^2, B) RAP <10 mmHg and SVI <35 ml/m^2, and C) RAP ≥10 mmHg. The RV echo indices were assessed for their ability to identify group B from C.

Results: With increased preload by passive leg elevation, cardiac output (CO), strain, SR-S, and SR-E increased significantly, while increased HR by atrial pacing increased only CO, SR-S, and SR-E. Under constant loading and HR, MIL and LEV increased CO by 20%, RV and LV strain by almost 20%, and SR-S and SR-E by almost 30% in both ventricles, with no differences between groups. In paper IV, echo indices of RV longitudinal function (such as TAPSE, S', FAC and strain) failed to distinguish group B from C, while all RV dimensional measurements could. By combining six RV echo indices into a novel score, the RV failure (RVF) score, significant discrimination between group B and C was found.

Conclusions: 1) Strain is preload- and HR-dependent while SR depends on HR. 2) MIL and LEVO have comparable effects on LV and RV systolic and diastolic function. 3) To assess RVF in LV disease, a single-parameter approach is inadequate and we propose a combination of six parameters into a novel RVF score.

Keywords: strain echocardiography, right heart catheterization, cardiac surgery, heart failure, levosimendan, milrinone, left ventricular function, right ventricular function, systole, diastole, preload, afterload, pacing, longitudinal function, ventricular dimensions, ventricular interdependence

Sammanfattning på svenska

Svårigheten med bestämning av hjärtats funktion är, att det föreligger ett komplicerat samspel mellan hjärtats pumpförmåga, dess grad av blodfyllnad i vilofasen, pumpmotståndet, som betingas av kärlbädden, och hjärtfrekvensen. Stort hopp har satts till nya ultraljudsmetoder som mäter hjärtmuskelns förkortning och avslappning (dess deformation). Vi ville undersöka om dessa metoder kunde utvärdera den direkta kontraktions- och avslappningsförmågan hos hjärtat oberoende av andra faktorer som blodfyllnad, pumpmotstånd och hjärtfrekvens.

För att öka hjärtfunktionen vid hjärtsvikt används ofta hjärtstärkande läkemedel. Två ofta använda är milrinon och levosimendan. Intressant nog föreligger mycket få tidigare jämförande studier av deras effekter på hjärtats funktion, och dessutom har de kommit till olika slutsatser. Genom att hålla fyllnadsgrad, kärlmotstånd och hjärtfrekvens konstanta ville vi jämföra de båda läkemedlens direkta effekt på hjärtfunktionen.

Vidare har det på senare tid visat sig vara betydligt svårare än vad man tidigare ansett, att bedöma högerkammarens funktion vid en samtidigt sviktande vänsterkammare, vilket var vårt fokus i det sista arbetet.

För de tre första arbetena undersökte vi patienter som genomgått öppen hjärtkirurgi genom att använda simultana mätningar från ultraljud och hjärtkateter. I arbete I utvärderade vi effekten på deformations-mätningar av isolerade ökningar i fyllnadsgrad, kärlmotstånd och hjärtfrekvens. I delarbete II och III lottades patienterna till milrinon eller levosimendan, och vi jämförde effekten på hjärtats inneboende kontraktions- och fyllnadsförmåga av läkemedlen. I delarbete IV studerade vi patienter med svår hjärtsvikt, vilka genomgått samtidig ultraljudsundersökning och hjärtkatetrisering, delade in patienterna i tre grupper baserade på grad av vänster- respektive högersvikt och jämförde ultraljudsdata från högerkammaren mellan grupperna.

Vi fann att även moderna metoder för mätning av hjärtats deformation är beroende av fyllnadsgrad och hjärtfrekvens, dvs. är belastningsberoende. Vi kunde visa att milrinon och levosimendan är likvärdiga i deras effekt på hjärtats inneboende pump- och fyllnadsförmåga. Slutligen såg vi att mätningar av högerkammarens funktion är svårbedömda vid samtidig vänsterkammarsvikt och att en korrekt bedömning av högerkammaren kräver en kombination av storleks-, geometri- och funktionsmått. Vi introducerade en ny poängskala, vilken vi hoppas kan underlätta framtida bedömningar av högerkammarfunktionen, i synnerhet vid en samtidig vänsterkammarsvikt.

List of papers

I. Fredholm M, Jörgensen K, Houltz E, Ricksten SE.

Load-dependence of myocardial deformation variables —A clinical strain-echocardiographic study.

Acta Anaesthesiol Scand. 2017;61(9):1155-1165.
DOI: 10.1111/aas.12954

II. Fredholm M, Jörgensen K, Houltz E, Ricksten SE.

Inotropic and lusitropic effects of levosimendan and milrinone assessed by strain echocardiography —A randomised trial.

Acta Anaesthesiol Scand. 2018;62(9):1246-1254.
DOI: 10.1111/aas.13170

III. Fredholm M, Jörgensen K, Houltz E, Ricksten SE.

Levosimendan or milrinone for right ventricular inotropic treatment? —A secondary analysis of a randomized trial.

Acta Anaesthesiol Scand. 2019;00:1-9. In press.
DOI: 10.1111/aas.13486

IV. Fredholm M, Ricksten SE, Bartfay SE, Karason K, Dellgren G, Bech-Hanssen O.

A multi-parameter echocardiographic approach offers better assessment of right ventricular function in patients with chronic left heart disease —A proposal for a new right ventricular failure score

Manuscript.

Contents

Abbreviations

A4C	apical four-chamber view
AAI	atrial demand pacing
ANCOVA	analysis of co-variance
ANOVA	analysis of variance
AS	aortic stenosis
AVR	aortic valve replacement
BSA	body surface area
cAMP	cyclic adenosine monophosphate
CO	cardiac output
CPB	cardio-pulmonary bypass
c_v	coefficient of variation
DAP	diastolic arterial pressure
DPAP	diastolic pulmonary arterial pressure
E_a	effective aortic elastance
eCVP	echocardiographically estimated central venous pressure
EDPVR	end-diastolic pressure–volume relationship
EDV	end-diastolic volume
E_{es}	ventricular (end-systolic) elastance
E_{pa}	effective pulmonary arterial elastance
ESPVR	end-systolic pressure–volume relationship
FAC	fractional area change
HR	heart rate
IQR	interquartile range
IVA	isovolumic acceleration
IVV	isovolumic velocity
LAAI	left atrial area index
LAI_{RV}	right ventricular loading adaptation index
LV	left ventricle
LVAD	left ventricular assist device
MAP	mean arterial pressure
ME 2CH	mid-esophageal two-chamber view
ME 4CH	mid-esophageal four-chamber view
MPAP	mean pulmonary arterial pressure
NT-proBNP	N-terminal prohormone of brain natriuretic peptide

NYHA	New York Heart Association
PAC	pulmonary artery catheter
PCWP	pulmonary capillary wedge pressure
PDE3	phosphodiesterase 3
P_{es}	end-systolic pressure
PKA	protein kinase A
PVR	pulmonary vascular resistance
PVRI	pulmonary vascular resistance index
RAAI	right atrial area index
RAP	right atrial pressure
RHC	right heart catheterization
RV	right ventricle
RV EDA	right ventricular end-diastolic area
RV ESA	right ventricular end-systolic area
RV SAX	right ventricular short axis diameter
RV sept	transversal length of the interventricular septum
RVD1	diameter of the basal inflow to the right ventricle
RVD3	the length of the right ventricle
RVF	right ventricular failure
RVOT prox	proximal right ventricular outflow tract diameter
RVSWI	right ventricular stroke work index
SAP	systolic arterial pressure
SD	standard deviation
SPAP	systolic pulmonary arterial pressure
SR	strain rate
SR-A	late diastolic strain rate
SR-E	early diastolic strain rate
SR-S	systolic strain rate
STE	speckle tracking echocardiography
SV	stroke volume
SVI	stroke volume index
SVR	systemic vascular resistance
SVRI	systemic vascular resistance index
TAPSE	tricuspid annular plane systolic excursion
TDI	tissue Doppler imaging
TEE	transesophageal echocardiography
TTE	transthoracic echocardiography
TV S'	tricuspid annular systolic velocity
VTI_{TR}	velocity time integral of a tricuspid regurgitation

1. Introduction

1.1 Autoregulation of heart function

The mammalian heart works with two serially connected circulatory systems that might be seen as each other's opposites. The right (pulmonary) side is a low-pressure system bringing blood low in oxygen and high in carbon dioxide back into the heart and then to the lungs, whereas the left (systemic) side is a high-pressure system bringing oxygenated blood from the lungs out into the body. The heart in a system like this needs to have separate right- and left-sided chambers, and is designed as a four-chambered heart.

1.1.1 An evolutionary perspective

The evolution of a four-chambered heart is closely linked to the development of endothermy (warm-blooded state), and is not only found in mammals, but also in birds, probably in the extinct dinosaurs, and more surprisingly in the ectothermic crocodiles [1-3]. With endothermy follows a higher demand for oxygenation, thus a higher hematocrit making the blood more viscous. This is proposed as one of several possible reasons why endothermy requires a much higher blood pressure on the systemic side, as opposed to in ectotherms. In fact, the pressures on the systemic side in endothermic animals is so high that it would harm the delicate lung tissue. Two separate circulatory systems with different pressures will solve this pressure problem and is probably the best reason for its development [1].

However, a circulatory system like this demands a near perfect and continuous balance (or feed-back) between the two sides, since otherwise, a congestion would quickly develop on either of the two systems if the two sides do not maintain equal output of blood (Fig. 1).

1.1.2 Two kinds of feed-back

The purpose of the feed-back is primarily to avoid edema from developing in the lungs in the case of an abruptly lowered left-sided performance. A lung edema

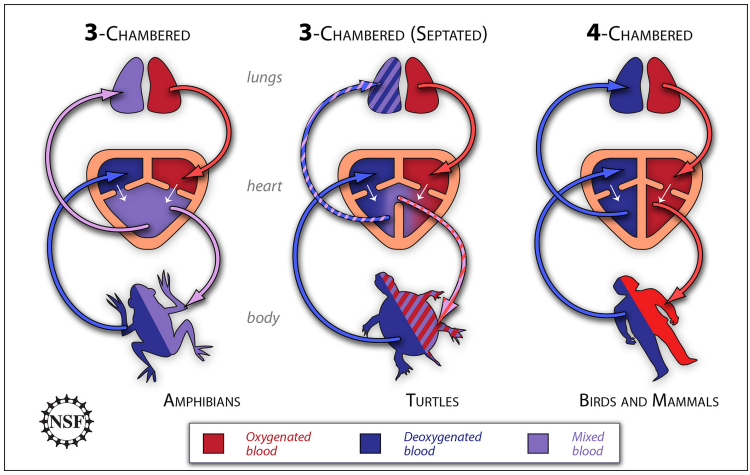

Figure 1. *The evolution of a four-chambered heart*
The successive development of an intraventricular septum is visible in turtles, who have an intermediate design of two incompletely separated ventricles. Any output difference between right and left sides can be equilibrated over the incomplete ventricular septum.
Courtesy of Zina Deretsky, National Science Foundation. Free for public use.

would be devastating for the animal, and the evolutionary drive to avoid this must therefore have been very strong.

To achieve a synchronized output between the left and right sides, two principal feedback mechanisms exists in the mammalian heart; 1) the homeometric autoregulation, or the Anrep effect, and 2) the heterometric autoregulation, commonly known as the Frank–Starling mechanism.

What von Anrep found already in 1912, was that an abrupt rise in blood pressure would lead to a successive increase in myocardial contractility, resulting in a lesser reduction of stroke volume than expected [4]. Though a progressive increase in intracellular Ca^{2+} levels has been observed, the exact mechanism for this is not completely clear. It seems to involve stretch receptors like integrins, leading to an increased release of angiotensin II [5].

During that same time, other researchers found proof of yet another intrinsic effect of the heart. One of them managed to sum it all up in a famous speech in Cambridge in 1915; Ernest Starling [6]. In short, the so-called Frank–Starling mechanism is the increased stroke volume delivered as a response to the ventricle being more filled and stretched at rest. Stretching of myocardial fibers will cause a greater number of actin-myosin cross-bridges to form, inducing a more pronounced shortening of the fibers. In that way it differs from the Anrep effect, which instead is a reaction to increased tension during contraction.

1.1.3 The importance of ventricular tension

We have now seen that there has to be an intrinsic autoregulation within the myocardium for a four-chambered heart to work properly. The homeometric autoregulation is linked to blood pressure and occurs during contraction (systole), while the heterometric autoregulation is linked to the ventricle's resting volume. Both these entities can be quantified as wall tension, which is equivalent to $P \times r/2h$, according to la Place's law [7], where P is pressure, r radius, and h wall thickness. It is this myocardial wall tension that is directly coupled to both autoregulatory mechanisms.

Two kinds of wall tension, or load, affect the myocardium; one at the start of the heart cycle, called preload, and one at the end, afterload. Preload thus is defined as the wall tension at the end of filling, i.e. end-diastole. On the other hand, afterload is the wall tension at the end of contraction, i.e. end-systole. In la Place's law, pressure (P) then corresponds to end-diastolic and end-systolic pressures, respectively.

In other words, the Anrep effect is a response to an increase in afterload, and the Frank–Starling mechanism to preload. Increasing any one of these loads would independently increase stroke volume (SV). One thing to keep in mind, though, is that there is a profound difference in the net effects on SV of the two loads. While increasing preload will increase SV, afterload will decrease it—the Anrep effect is there only to attenuate the decrease. To be even more accurate (see paragraph 1.1.8), the Anrep effect increases the intrinsic myocardial contractility, i.e. the degree of contraction at a certain preload and afterload, whereas the Frank–Starling mechanism increases SV.

1.1.4 Can we measure wall tension or load?

Unfortunately, measuring load by its proper definition (wall tension) in a clinical setting is difficult and time consuming. Therefore, in most clinical situations, an approximation is done by using surrogate variables, such as ventricular end-diastolic and end-systolic dimensions or their related pressures. The pressure surrogates used for preload assessment are pulmonary capillary wedge pressure (PCWP) for the left ventricle (LV) and central venous pressure (CVP) for the right ventricle (RV). End-systolic pressure can be approximated as 0.9 × systolic arterial pressure (SAP) for the LV but is closer to mean pulmonary arterial pressure (MPAP) for the RV.

A parameter more directly correlated to afterload is the effective arterial elastance. Its strength is that it incorporates all elements impeding upon ventricular ejection—denoted outflow impedance. The two major elements of elastance (outflow impedance) are; 1) vascular resistance, i.e. the peripheral resistance to flow stemming from arterioles (resistance vessels), and 2) characteristic impedance, i.e. the distensibility of the large arteries. The formulas for elastance have been adapted to clinical settings

from the original definition and differ somewhat between the LV and RV (Table 1). Both have been shown to correctly assess aortic (E_a) and pulmonary arterial (E_{pa}) elastances and to be valid measures of outflow impedance [8, 9].

Variable	Symbol	Formula
Effective aortic elastance (LV)	E_a	$0.9 \times SAP/SV$
Effective pulmonary arterial elastance (RV)	E_{pa}	$(MPAP - PCWP)/SV$
Systemic vascular resistance	SVR	$(MAP - CVP)/CO$
Pulmonary vascular resistance	PVR	$(MPAP - PCWP)/CO$

Table 1. *Summary of the variables related to ventricular outflow impedance*
SAP, systolic arterial pressure; SV, stroke volume; MPAP, mean pulmonary arterial pressure; PCWP, pulmonary capillary wedge pressure; MAP, mean arterial pressure; CVP, central venous pressure; CO, cardiac output.

1.1.5 Ventricular interdependence

So, the right and left sides of the heart are more or less synchronized in their performance through the feed-back mechanisms of preload and afterload (at least in a healthy heart). But this is not the entire truth, and there is evidence of other connections between the two ventricles—the first report on this written already in 1910 by Bernheim [10]. The syndrome that he described was that of RV failure in patients with a hypertrophic LV. In essence, the sharing of anatomical structures by both ventricles holds the explanation to this phenomenon, called ventricular interdependence: 1) a common and confined space within the pericardium, 2) the interventricular septum, and 3) sharing of muscle fibers. This interdependence is often separated into a diastolic and a systolic part [11].

Let us look at a dilated RV, to start with. Assuming that, whatever the reason, its end-diastolic volume (EDV) is increased. The dilation reduces the volume available for the LV, as a natural consequence of the confined volume within the pericardium and the leftward displacement of the common septum. The resulting small LV EDV (low LV preload) results in a smaller SV. A balance between both sides is thereby achieved, i.e. diastolic interdependence [12].

On the other hand, systolic interdependence is defined as the contribution of contractile function from one ventricle to the other. Primarily, it is mediated by the interventricular septum and its ability to shift position between left and right, but sharing of muscle fibers between the ventricles also contributes. For instance, in severe isolated RV failure, the septum will be displaced from the left in diastole to the right in systole, thereby assisting the RV. It has been estimated that 80% of RV contractile function emanates from the LV through this interdependence [11, 13].

1.1.6 The staircase

Finally, heart rate (HR) also affects myocardial contractility, such that for every increase in HR (up to about 120 beats/min), the contractility increases as well. This, the third and final autoregulatory mechanism, is called the Treppe or staircase phenomenon, but is mostly referred to by the name of its discoverer as the Bowditch effect. He described it in frog's heart already in 1871 [14], but it has since been confirmed also in humans. Although the exact mechanism is still not clear, changes in cellular calcium handling may be involved. The Bowditch effect might contribute to as much as 40% of the increased cardiac output in exercise [15, 16].

1.1.7 Summing it up

The evolution of a four-chambered heart demanded a simultaneous development of feed-back systems to keep a balance in output between right and left sides of the circulation. In fact, most symptoms arising in heart failure due to cardiac disease are secondary to a non-functioning feedback.

Delivering blood to the body is the main purpose of the heart, and the volume delivered per minute, the cardiac output (CO), is simply the product of HR and SV. On the other hand, SV is the result of a complex interaction of preload, outflow impedance, and contractility (Fig. 2)—the latter in turn affected by afterload and heart rate, as well as adrenergic hormones, calcium, hypoxia, disease, drugs etc.

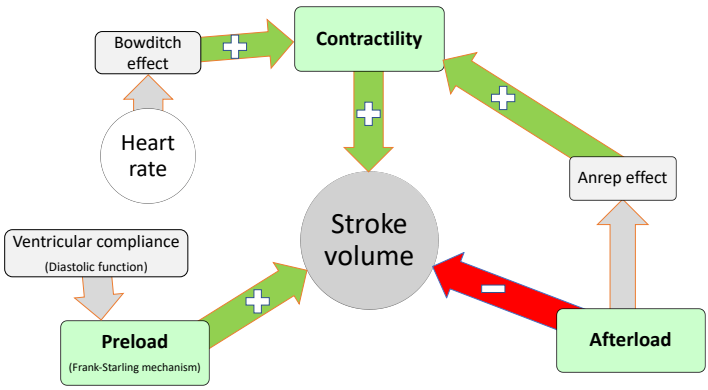

Figure 2. *Summary of the different variables affecting stroke volume*

The main focus of this thesis is on myocardial contractility. In all of papers I–III it is a primary outcome, while in paper IV it is not measured as such, but is rather the underlying issue that that final paper is dealing with. Before getting into more detail,

we need to introduce three terms that are in everyday use whenever referring to cardiac function: inotropy, lusitropy, and chronotropy.

Contractility and inotropy are synonyms. Simply put, it is the force by which the myocardium contracts, equaling the systolic function at a certain heart rate, pre- and afterload. Anything that increases contractility has a positive inotropic effect.

Lusitropy is defined as active myocardial relaxation, and is an important factor for diastolic function. The muscle fibers relax when cytoplasmic calcium is pumped back into the endoplasmic reticulum and is therefore an energy-consuming process, just as contraction. Different cardiac pathologies can reduce the lusitropy, thus decreasing ventricular distensibility. The decreased distensibility impairs ventricular filling at a certain preload, in turn yielding a lower SV. Anything that increases relaxation has a positive lusitropic effect.

Finally, chronotropy is equal to heart rate. Anything that increases heart rate is called a positive chronotropic agent.

1.1.8 The ventricular pressure–volume relationship

By simultaneously measuring ventricular pressure versus volume at end-systole over a range of different preloads, myocardial contractility can be determined. This was first showed in 1973 by Suga and Sagawa in canine hearts [17], but has since been reproduced in vivo also in humans [18]. This, the end-systolic pressure–volume relationship (ESPVR), also denoted as ventricular elastance (E_{es}), is still the most accurate estimate of myocardial contractility (inotropy). It presents as a straight line cutting through all end-systolic pressure-volume points (corresponding to point A in Fig. 3) that have been collected from all the different loops. The slope is a load-independent measure of contractility (depicted by the blue line in Fig. 3) [19].

Within the loop, the end-systolic pressure-to-stroke volume ratio (P_{es}/SV) can be determined (red line in Fig. 3). This is in fact the effective arterial elastance (E_a) described in paragraph 1.1.4, and constitutes the ventricular outflow impedance. On the other hand, calculating afterload needs end-systolic pressure (point A in Fig. 3) to be inserted in la Place's law ($P_{es} \times r/2h$, paragraph 1.1.3).

Finally, the end-diastolic pressure–volume relationship (EDPVR, from B to C in Fig. 3), representing ventricular filling, can also be determined—the curvilinear slope being inversely correlated to ventricular compliance, meaning that a steeper EDPVR slope indicates decreased ventricular compliance [20]. This is the result of an impaired ventricular lusitropy, with or without a stiffer wall due to a structural adaptation (such as hypertrophy and/or collagen formation).

By changing the preload, outflow impedance and inotropy separately, the pressure–volume loops will show us that an increased preload results in a greater SV, but

on the other hand (in the absence of any Anrep effect) an increased outflow impedance would result in a smaller SV. Lastly, any agent increasing inotropy will create a steeper ESPVR slope (Fig. 4).

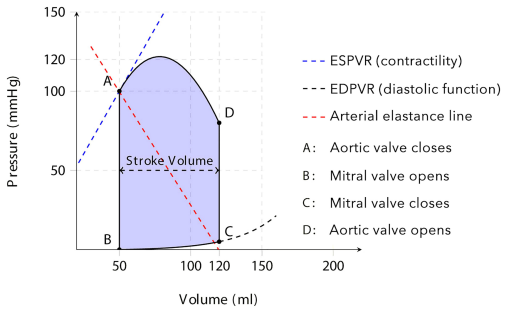

Figure 3. *Pressure–volume loop of the left ventricle*
The ESPVR (end-systolic pressure–volume relationship) and EDPVR (end-diastolic pressure–volume relationship) lines are derived from several pressure–volume loops recorded at altering preloads. The blue ESPVR line is the LV elastance—a load-independent measure of LV contractility. The red line (from C to A) indicates the end-systolic pressure to stroke volume relationship, or the effective aortic elastance, E_a—a direct measurement of LV outflow impedance and correlated to afterload. The black EDPVR line is the LV compliance—a measure of diastolic function.
Modified from © C. Jake Barlow at LITFL, http://www.partone.litfl.com
Creative Commons BY-NC-SA 4.0 license.

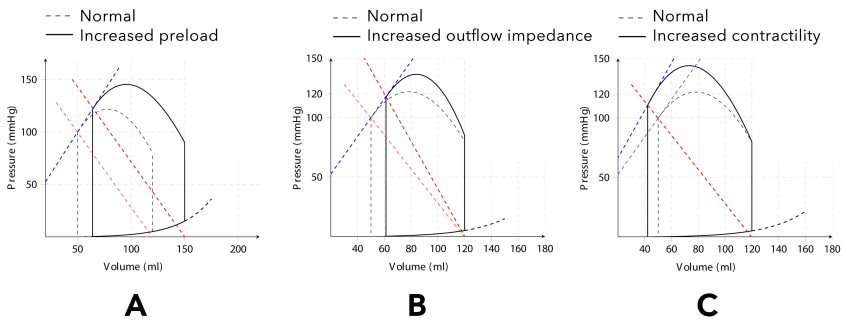

Figure 4. *Pressure–volume loops of the LV showing effects of altering load and contractility*
Panel A: preload is increased, resulting in a larger SV with unchanged contractility (shown by the unaltered ESPVR line). Panel B: outflow impedance is increased, resulting in a steeper E_a line (increased effective arterial elastance) and a smaller SV. This panel is true only if contractility would remain constant, because the presence of an Anrep effect would attenuate the decrease in SV by a steeper ESPVR line (not shown). Panel C: contractility is increased by an inotropic agent, increasing ESPVR, resulting in a larger SV.
Modified from © C. Jake Barlow at LITFL, http://www.partone.litfl.com
Creative Commons BY-NC-SA 4.0 license.

In summary, the gold standard for estimating load-independent LV myocardial contractility, in vivo, is to analyze LV pressure-volume loops at various levels of preload. Such an assessment of myocardial contractility is, however, not readily available in the clinical setting. Thus, there is a need for non-invasive evaluation of myocardial contractility in the clinical arena.

1.2 Myocardial deformation analysis

Echocardiography has become the dominant diagnostic method to evaluate cardiac pathology, since it is a readily available, non-invasive, bedside tool. The development is ongoing with new techniques constantly added to the arsenal. This thesis is focused on myocardial deformation analysis, which is one of the more recent developments. Terms like strain and strain rate are the essence of deformation analysis, and this chapter will try and explain the concept [21].

1.2.1 Finding the Holy Grail

As shown above, stroke volume (SV) is the end product of a complex interplay of heart rate, diastolic filling, contractility, and effective arterial elastance (outflow impedance). In a clinical diagnostic situation, contractility is often the sought-after property of the heart, since this is where any cardiac disease will strike. The ESPVR that we have encountered is definitely load-independent, but it is too invasive and difficult to be used in everyday clinical work. Finding an echocardiographic load-independent method that actually measures contractility would be of great value. When introduced, deformation analysis was proposed as a probable candidate, but subsequent studies on its load-dependence have shown divergent results [22-30].

Papers I and IV in this thesis deals with the load-dependency problem—the first paper focusing specifically on the load-dependency of the various LV deformation variables, while the fourth describes the importance of various echocardiographic variables for the evaluation of RV function in patients with left heart disease.

1.2.2 What is deformation, strain and speckle tracking?

During systole and diastole, the myocardium is undergoing shortening and lengthening—this is called deformation. It occurs along three dimensions: during systole, the ventricles will 1) shorten longitudinally (i.e. from base to apex) and 2) circumferentially, while 3) in the radial direction LV wall thickness will increase. Naturally, the

reverse is happening in diastole. Throughout this thesis, we have only measured longitudinal deformation, because it is the most used clinically and is shown to have the best reproducibility of the three [31].

Strain (often abbreviated ε) is no more than a measure of the relative change in length of a segment of the myocardial wall. If a rubber band is stretched from four to six centimeters, it has increased in length by 50%, which is the same as a strain of +50% (compared to the reference state). A myocardium that contracts during systole will have a negative longitudinal strain (equal to shortening). Normal LV longitudinal strain is around −20%, and for the RV −25%, but they vary greatly with gender, age, and wall segment studied [32, 33].

Speckle tracking echocardiography (STE) is one of two methods for collecting deformation data, the other being tissue Doppler imaging (TDI). Both methods have their respective strengths and weaknesses. Tissue Doppler imaging has the advantage of a much higher image framerate, but as with all Doppler measurements in general, it is dependent on the angle of insonation. STE, an angle-independent technique using image post-processing [34], has several advantages compared to TDI: less time-consuming to perform, lower interobserver variability and less noise-sensitivity [35].

In any 2-dimensional ultrasound image, because of interference and reflections, a pattern of irregularities in the grey scale will occur. Each myocardial region has a unique pattern (its "fingerprint") and by identifying and following different markers of this pattern, called speckles, the software can calculate the change in length (strain) of that specific region (Fig. 5) [36]. In a recent review, promising results have been shown for myocardial wall deformation imaging by STE in a peri-operative setting in respect to adverse outcome after surgery [37].

1.2.3 Introducing the strain rates

Looking at a strain curve from one heart cycle, three slopes and one peak can be identified, the peak being the (systolic) strain of that segment. The slope leading up to the peak is the contraction in systole, and the steeper the slope, the more rapid the contraction. The slope $\Delta L/T$, where ΔL is the difference in length (= strain) and T is time, gives us a measure of velocity with the unit s^{-1}. This is the strain rate (SR) or the speed by with deformation occurs. In systole, this is an equivalent of the velocity of contraction, and the systolic strain rate is often designated SR-S.

During diastole, there will typically be two slopes with a brief plateau in-between. The reason: diastole is biphasic and comprises of an early phase of ventricular relaxation, and a late phase of ventricular lengthening caused by atrial contraction. These two different strain rates are often referred to as SR-E and SR-A, respectively (Figs. 6 and 7).

In the case of diastolic dysfunction, the relation of SR-E to SR-A will be altered in a manner similar to the E/A-relationship from a mitral valve Doppler [38].

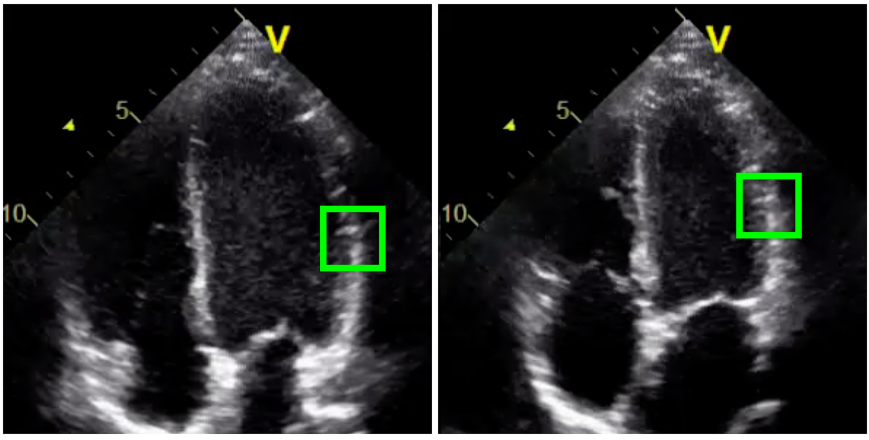

Figure 5. *Speckle tracking*
The speckle tracking method means post-processing of a 2-dimensional echocardiographic image. The software identifies unique patterns ("speckles") in the grayscale of the myocardium, which are then followed throughout the cardiac cycle. The movements of several speckles are integrated to yield strain and strain rate for the specific segment. Apical 4-chamber view from a trans-thoracic echocardiography. Left panel in diastole and right in systole.

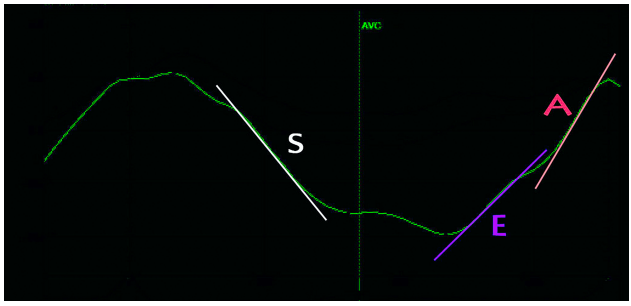

Figure 6. *Strain rate derivation*
From the strain curve, three slopes can be identified, and their derivations correspond to each of the three strain rates (SR). S *is systolic strain rate, SR-S. From the biphasic diastole two strain rates can be calculated:* E *is early diastolic SR (SR-E) during ventricular relaxation (affected by the ventricle's lusitropy) and* A *is late diastolic SR (SR-A), i.e. myocardial lengthening during atrial contraction. AVC in the picture denotes aortic valve closure.*

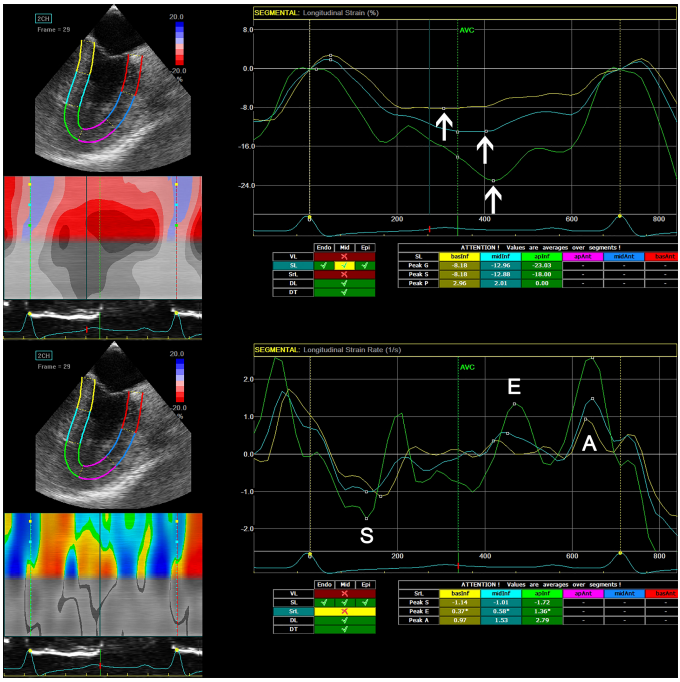

Figure 7. *Strain and strain rate curves*
Top panel: Strain curves recorded from the LV inferior wall in a mid-esophageal 2-chamber view. The wall is automatically divided into three segments; basal, mid, and apical, represented by the three individual curves. The peak negative points on the curves (marked by arrows) are the segmental peak strain values. The mean of the three will represent inferior wall strain.
Bottom panel: Corresponding strain rate curves recorded during the same heart cycle. The peak segmental strain rates are denoted in the figure; S *for SR-S,* E *for SR-E and* A *for SR-A.*

1.2.4 Interpreting the values

Strain and its derivation (SR) are defined as changes in length from baseline, as mentioned previously. Thus, during systole, the longitudinal shortening that occurs in both ventricles yields negative values on both longitudinal strain and SR—and, the more negative values, the better systolic function. So far, so good.

Diastole could be defined as the return of strain to baseline, merely representing a slope on the strain curve. Therefore, we will find no peak strain in diastole (even though there recently have been developed a concept of diastolic strain, I will leave that behind). Derivation of the strain curve gives us the SR curve, which will have three peaks, one systolic and two diastolic. The diastolic longitudinal SR peaks, SR-E and SR-A, are both positive since they represent a lengthening of the muscle fibers back to baseline. The more positive value, the faster the relaxation.

The height of SR-E measures the velocity of the (energy-dependent) active myocardial relaxation (lusitropy) of the ventricle, which is an important component of diastolic function. An impaired myocardial relaxation, caused by e.g. myocardial ischemia, will yield a lower SR-E, in turn making atrial contraction more important for ventricular filling, resulting in a higher SR-A [39].

1.3 The enigmatic right ventricle

When comparing the two ventricles, major differences are revealed. Looking at the RV, the most important characteristics in relation to the LV are:

1) Working with much lower pressures, having a flatter pressure–volume curve
2) Thinner wall and a lower effective arterial elastance (impedance)
3) Much more sensitive to changes in RV outflow impedance
4) More complex 3-dimensional geometry

Together, these characters make the RV harder to study [40].

Firstly, the geometrical complexity makes evaluation of its function more difficult, especially by echocardiography.

Secondly, the functional characteristics (no. 1–3 above) makes it more dependent on LV function than the other way around. Since its pressure is lower, it is more easily compressed (a more pronounced diastolic interdependence). Also, the higher impedance-dependency will reduce its SV to a much greater extent compared to the LV at an equal rise in outflow impedance. For example, in a situation of LV dysfunction, the raised LV filling pressure (preload) will transmit across the pulmonary vascular system resulting in an increased RV outflow impedance, thus lowering its SV as a response [41]. Recent findings suggest that this impedance sensitivity might, at least with progressing LV disease, be the result of systolic ventricular interdependence [42].

1.3.1 Dimensional parameters

As RV geometry is more complex than the cone-shaped LV, several echocardiographic measures of RV dimensions have been presented. I will not go into these in detail, but it is worth pointing out, that there is now a consensus on how to measure RV dimensions, as also expressed in recent guidelines [43, 44].

Commonly used measurements from the guidelines and used in this thesis are: proximal RV outflow tract diameter (RVOT prox), diameter of the basal inflow to the RV (RVD1), the length of the RV (RVD3), and RV end-diastolic and end-systolic areas (EDA and ESA, respectively). From the latter, the fractional area change (FAC)

is calculated as FAC = (EDA − ESA)/EDA. Not included in the guidelines, but often referred to, are two cross-sectional dimensions: the RV short axis diameter (RV SAX) and the transversal length of the interventricular septum (RV sept), both measured in a short axis view.

1.3.2 Functional parameters

Among the functional parameters that are included in the guidelines, deformation analysis is one. The principles for measuring RV strain and strain rate are the same as for the LV. One possible difference, according to some authors, is perhaps that the interventricular septum should be excluded when assessing global RV strain, since it is highly integrated in the LV contractile mechanism [45]. In this thesis, only the RV free wall longitudinal strain and SR are therefore referred to.

As for the rest of the functional parameters, they are all measured at the lateral tricuspid annulus, either as two-dimensional or Doppler measurements. The distance (in mm throughout this thesis) by which the tricuspid annulus moves towards the apex during systole is defined as the tricuspid annular plane systolic excursion (TAPSE) [46, 47]. The speed by which this movement occurs can be measured through TDI and is called the tricuspid annular systolic velocity (TV S') [48]. The unit for TV S' is cm/s.

Before systole begins, there is a brief period of myocardial contraction without any detectable effect on the volume of the ventricle. This period is called the isovolumic contraction and in recent years, there has been some interest in this phase as a possible load-independent measure of contractility. Two parameters seem promising in the assessment of RV contractility: myocardial acceleration during isovolumic contraction (or simply isovolumic acceleration, IVA) and peak velocity during isovolumic contraction (isovolumic velocity, IVV) [49, 50]. Both can be identified on the TDI curve of the tricuspid lateral annulus (Fig. 8).

A limitation of commonly used RV functional parameters is that they measure only longitudinal function. However, in chronically elevated afterload, as in pulmonary hypertension or LV failure, studies have shown that longitudinal function alone might not accurately assess RV contractility [51-53]. Radial function will have a proportionally greater impact in this situation. This is probably due to RV adaptation to load. A well-adapted RV will maintain its contractility by hypertrophy. Conversely, insufficient adaption will lead to RV failure, which is characterized by increased CVP, RV dilation, a more spherical form, and development of severe tricuspid regurgitation. Thus, adding measurements of RV dimensions and geometry to the functional parameters will provide a more robust assessment of RV function.

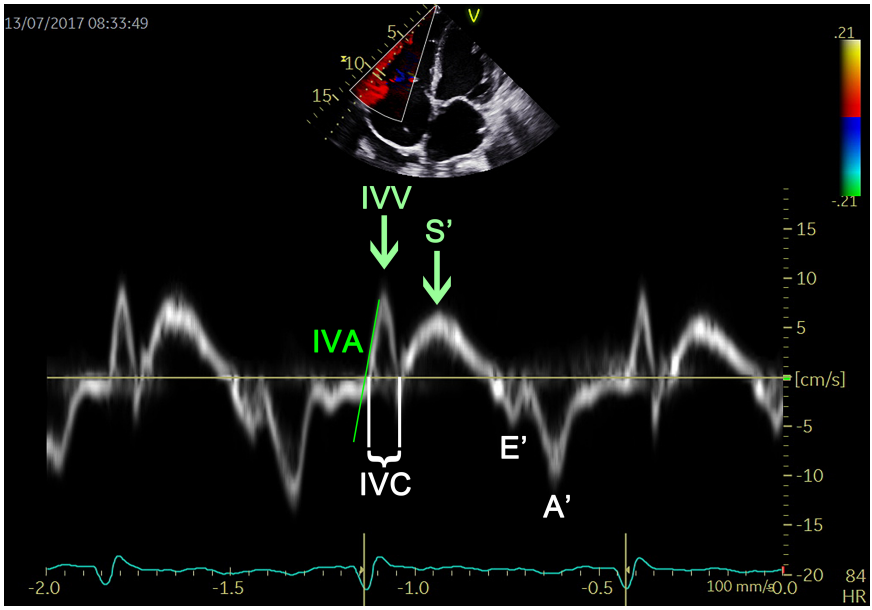

Figure 8. *Tissue Doppler of the lateral tricuspid annulus*
Recording from the apical 4-chamber view. Upward movements (toward the probe) represent systolic motion. IVC is the isovolumic contraction and the maximum speed during this period is the IVV (isovolumic velocity). The acceleration during IVC is shown as the derivate IVA (isovolumic acceleration), which is calculated as IVV/ΔT, where ΔT is the start-to-peak velocity time of the IVC.
S' denotes peak velocity of the tricuspid annulus during systole. The diastolic velocities E' and A' of the annulus are included for clarity (in this case E' ≪ A' would suggest diastolic dysfunction).

1.4 The concept of inodilation

Finally, before getting into aims, methods, and results of this thesis, it is time to introduce the inodilators. They belong to a family of inotropic agents often used in critical care for treating acute heart failure. An inodilator is a drug that increase SV by combining two mechanisms, increased contractility (inotropy) and reduced outflow impedance (through vasodilation).

1.4.1 Calcium

Within all cells of the body, the calcium ion (Ca^{2+}) is scarce but important. It is involved in a plethora of intracellular processes, all starting with a sudden burst in the

intracellular Ca^{2+} concentration. Triggered by external stimuli, Ca^{2+} channels in the cell membrane suddenly open and Ca^{2+} starts flooding down its concentration gradient from depots outside or inside (the endoplasmic reticulum) the cell into the cytoplasm itself. In muscle cells, Ca^{2+} is responsible for contraction. In fact, the mechanism of contraction is so completely dependent on Ca^{2+} that without it, there cannot be any. As a consequence, anything that increases the intracellular Ca^{2+} concentration will result in a (more forceful) contraction. Reciprocally, to start relaxation, Ca^{2+} has to be actively removed from the actin-myosin filaments, responsible for the contraction, back into the endoplasmic reticulum. This removal, plus the subsequent transport out of the cytoplasm, are the reasons for diastole being an energy consuming process.

1.4.2 The phosphodiesterase enzyme

Common for all cells is a tiny molecule called cyclic adenosine monophosphate (cAMP), working as one of several second messengers—molecules responsible for the communication between cell surface receptors and intracellular proteins [54].

The intracellular concentration of cAMP in myocytes can be increased by catecholamine-induced β_1-receptor stimulation, increasing the formation of cAMP from adenosine triphosphate (ATP). cAMP is degraded back to ATP by phosphodiesterase enzyme 3 (PDE3, Fig. 9), so by inhibiting PDE3 the amount of intracellular cAMP will increase. This increase will in turn lead to different outcomes depending on which cell type it is taking place in. In the muscle cells of arterioles, relaxation is the result, leading to vasodilation. In the myocytes of the heart, contractility and relaxation will be enhanced. In other words, the PDE3 inhibition results in a combined inotropic and lusitropic effect.

In cardiac myocytes, increasing cAMP will activate protein kinase A (PKA) leading to both an increased influx of Ca^{2+} into the cell and a more effective Ca^{2+} reuptake into the sarcoplasmic reticulum. Thus, in systole, a higher intracellular Ca^{2+} concentration leads to faster and stronger contraction. Then, in diastole, the intracellular Ca^{2+} concentration will decrease faster, leading to a faster relaxation (Fig. 9). In arterioles, on the other hand, the vasodilatory effect is mediated through myosin light chain kinase, a protein involved in contraction and which is inactivated by cAMP.

From the above, we can conclude that increasing cAMP will enhance inotropy, lusitropy and vasodilation; i.e. inodilation. Since cAMP is degraded back to ATP by PDE3, inhibiting this enzyme will increase the intracellular cAMP concentration. This is in fact the mode of action for most inodilating drugs (Fig. 9) [55].

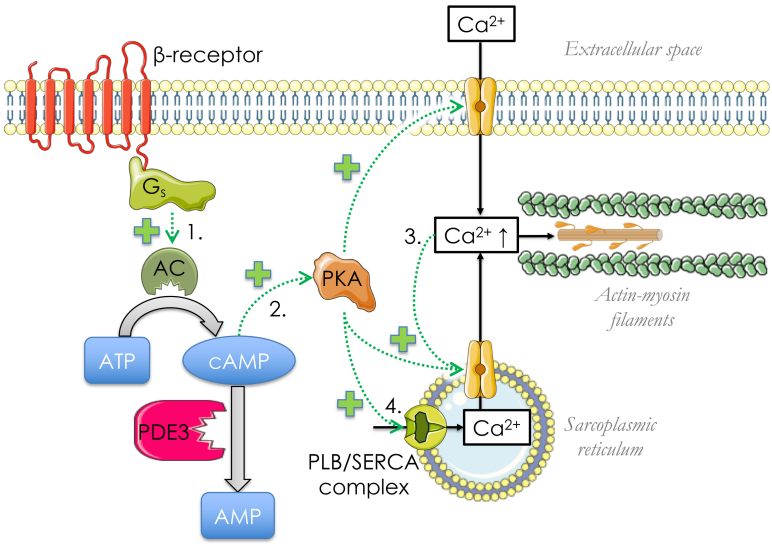

Figure 9. *The intracellular response to β-adrenergic stimulation*

1. *The β-adrenergic receptor is coupled to a G_S protein (stimulatory G protein), meaning that whenever activated by the binding of a catecholamine (e.g. epinephrine), the receptor/G_S protein complex will increase cAMP production by stimulating the enzyme adenylyl cyclase (AC).*

2. *The increased concentration of cAMP in turn activates protein kinase A (PKA), which starts phosphorylating several target proteins, in this case Ca^{2+} channels in both the cell membrane and the sarcoplasmic reticulum, leading to an influx of Ca^{2+} into the cytoplasm.*

3. *Increased intracellular Ca^{2+} concentration further stimulates Ca^{2+} channels in the sarcoplasmic reticulum to open and release even more Ca^{2+} into the cell.*

4. *Another target for PKA is the regulator protein phospholamban (PLB), that normally inhibits the pump responsible for Ca^{2+} re-uptake into the sarcoplasmic reticulum. Phosphorylation of PLB will inactivate it, so that the pump, called SERCA (sarcoplasmic reticulum Ca^{2+}-ATPase), works faster, pumping Ca^{2+} away from the cytoplasm back into the sarcoplasmic reticulum, leading to relaxation.*

1-3. *in the picture are inotropic and* 4. *is lusitropic.*
Inhibiting phosphodiesterase 3 (PDE3), the enzyme responsible for degrading cAMP back to ATP, will increase cAMP concentration and lead to both inotropy and lusitropy.
Picture by the author using contents from © Les Laboratoires Servier, downloaded at https://smart.servier.com/, Creative Commons BY 3.0 license.

1.4.3 Milrinone

Acting as a PDE3 inhibitor, milrinone was developed in the early 1980s from its predecessor amrinone [56, 57]. The effects are well documented and explainable by increased intracellular cAMP; inotropy, lusitropy, and vasodilation. Compared to adrenergic hormones (catecholamines like epinephrine, norepinephrine, dopamine, and dobutamine), the vasodilatory effect is more profound [58]. The reason being that adrenergic hormones stimulate both β- and α-receptors—the latter more common in peripheral vessels and acting by inhibition of cAMP production.

Today, milrinone is included in both the European and American guidelines for treatment of acute heart failure [59, 60], a condition where treatment is based on three principles: diuretics, vasodilators, and inotropes. Together with other inotropes, milrinone not just shares the indication (hypoperfusion combined with hypotension), but also concerns about long-term efficacy and mortality effects [61].

Milrinone is sold under the brand names Primacor® and Corotrop®.

1.4.4 Levosimendan

Another class of inodilators are the calcium sensitizers. Their primary effect is increasing the sensitivity of the contractile apparatus to Ca^{2+}, giving these drugs pure inotropic characteristics. Their mode of action is to alter the configuration of troponin C, the Ca^{2+}-binding protein within the contractile apparatus. By this alteration, the potency of troponin C compared to its counterpart—the inhibitory troponin I—is increased, yielding a faster and stronger contraction. The increased binding of Ca^{2+} to troponin C has raised concerns whether the calcium sensitizers will, in fact, impair the removal of Ca^{2+} from troponin back to the endoplasmic reticulum and thus induce a negative lusitropic effect [62].

Around 15 years after the registration of milrinone, the calcium sensitizer levosimendan was developed [63, 64]. As it is not a pure calcium sensitizer, but acts partly as a PDE3 inhibitor, it also has a positive lusitropic effect [65, 66] that might counteract the potential negative effect seen with other calcium sensitizers (see above). In a clinical study, Jørgensen et al. showed that levosimendan, in fact, shortened time for isovolumic LV relaxation, suggesting a positive lusitropic effect [67]. However, the question remains, whether there is a difference between the two inodilators, levosimendan and milrinone, with respect to early diastolic ventricular relaxation.

Additionally, levosimendan is also a potent vasodilator by opening two different kinds of potassium channels in vascular myocytes, leading to hyperpolarization, causing decreased Ca^{2+} influx through voltage-dependent Ca^{2+} channels, and subsequently smooth muscle relaxation. This vasodilation occurs both in arterioles and veins, reducing both pre- and afterload [68, 69].

The presence of an active metabolite, OR-1896, with a long (>80 hours) half-life, gives levosimendan a prolonged action of several days [70]. Furthermore, compared to pure PDE3-inhibitors, the interaction with troponin C is shown to give inotropic effects without increasing oxygen consumption, a supposed benefit in the treatment of acute heart failure [71]. Until now, over 500 randomized studies on levosimendan have been performed, most of them versus placebo or dobutamine, but just a handful versus milrinone! A review in 2012, including 45 studies, found that levosimendan "might reduce mortality in cardiac surgery and cardiology" [72]. Despite these recent findings, levosimendan is not yet approved in the United States. It is, however, included in the European guidelines for treatment of acute heart failure, with the same indications as milrinone (hypoperfusion combined with hypotension) [59].

Levosimendan is sold under the brand name Simdax®.

1.5 Summary and previous research

From what has been shown in the introduction, the following conclusions can be made:

- Cardiac output (CO) is the result of a complex interplay of several factors, with contractility and relaxation being two of them.
- Measuring contractility and relaxation is difficult, since most measurements of heart function are confounded by the heart's loading conditions and heart rate.
- Contractility and relaxation can be increased by inotropic drugs, but most inotropic drugs also act by reducing afterload, having an additive effect on CO.
- If we want to compare the effects on contractility and relaxation of inotropic drugs, we need to keep loading conditions and heart rate constant.
- When correctly assessing RV function, the influence of LV function might need to be considered, and a multi-parameter echocardiographic approach is probably required.

Measuring contractility and relaxation through deformation analysis is promising, but studies on its load-dependency are not uniform. Strain is shown to be dependent on both pre- and afterload in several studies, while systolic SR findings are inconsistent and diastolic SR data even lacking [22, 26, 28-30]. We wanted to address this lack of information in our first paper.

Using deformation imaging, the two commonly used inodilators milrinone and levosimendan were compared in our second and third papers for their effects on LV and RV function. Few previous randomized, controlled trials have assessed the drugs head-to-head, and none of them used controlled loading conditions and heart rate [73-78]. To our knowledge, our studies are the first to assess these drugs in respect to LV and RV contractility and relaxation, keeping preload, afterload, and heart rate

constant. They are also the first to compare the two drugs in respect to LV early relaxation (SR-E).

Finally, since the RV is strongly influenced by increased afterload, any reduction in LV function will affect the RV and decrease its output. As previously mentioned, the RV can adapt to this situation and uphold an adequate function, preventing forward failure. In the reversed scenario, with no or limited RV adaptation to increased load, the RV will dilate and change into a more spherical shape, leading to a less effective contraction and finally RV failure. Foreseeing the development of RV failure in patients with LV dysfunction is difficult and many studies have shown that no single echocardiographic parameter is predictive enough. At least the commonly used echocardiographic variables relating to RV longitudinal function seem inadequate [79-81].

In patients with severe LV failure, implantation of a left ventricular assist device (LVAD) can be a solution both as a long-term therapy when all other treatments have failed, or as a bridge to transplantation. These cases have to be thoroughly evaluated in respect to their RV function, since the RV will receive a much higher venous return. Thus, any RV failure that might be masked by the low-CO syndrome present due to LV failure in these patients, might worsen after LVAD insertion. Prediction of RV function in these patients is known to be difficult and reliant on a combination of RV measurements [80]. A possible echocardiographic strategy for assessing RV function could be to use a score, integrating measurements of RV longitudinal function, size, geometry, adaptation to load, estimation of CVP, and grading of tricuspid regurgitation.

Still, this is an area of ongoing research, and our last paper will hopefully add some more insight on how to evaluate RV function in concomitant LV failure.

2. Aims

From the above arguments and known gaps in previous research, the aims of this thesis were defined, one for each of the four included papers:

I. To evaluate the dependency of LV deformation parameters (strain and strain rate) on isolated changes in preload, afterload, and heart rate, and to describe the effects of these changes.

II. To compare the effects on LV contractility and relaxation of two commonly used inodilators, levosimendan and milrinone, in patients after cardiac surgery at controlled heart rate, preload, and afterload.

III. To compare the effects on RV contractility and relaxation of the two inodilators levosimendan and milrinone in patients after cardiac surgery at controlled heart rate and preload.

IV. To evaluate whether classic echocardiographic RV dimensional and functional parameters, as well as RV adaptation to load, estimation of CVP, and grading of tricuspid regurgitation, are able to detect RV systolic dysfunction in the presence of LV forward failure, also introducing a novel echocardiographic RV failure score.

3. Patients and methods

The first three papers are fairly coherent around a common methodology, similar protocols and an overlap of patients. They will therefore be described together. The fourth paper is retrospective—the first three all prospective—but it differs also in terms of investigators, methods, and patients.

Throughout all the papers, both hemodynamic and echocardiographic measurements were performed in a similar way and will therefore be described together. Worth pointing out is that all included patients in the thesis (except for three echocardiographic drop-outs due to bad image quality) were assessed with this combination of invasive and non-invasive data, which is one of the major strengths of the thesis. Another strength is the way we were able to control confounding physiological factors (preload, afterload, and heart rate), in the assessment of ventricular contractility (inotropy) and early relaxation (lusitropy) in Papers I-III.

3.1 Papers I–III

We included patients admitted to our department for open-heart surgery due to aortic stenosis (AS). The studies were undertaken during the immediate post-operative period with patients still intubated under mechanical ventilation. Since AS creates a chronically elevated afterload, the increased stroke work imposed on the LV will make it hypertrophy. As a result, these patients require a higher than normal LV end-diastolic filling pressure to attain normal LV end-diastolic volume, i.e. they have a LV diastolic dysfunction [82]. Since one of the aims of paper II–III was to compare the lusitropic effects of milrinone and levosimendan, this diastolic dysfunction was the main reason for choosing AS patients. On the other hand, we included only patients with normal or just mildly reduced RV and LV systolic function, setting the cut-off for exclusion to a LV ejection fraction of <50%.

Also, using post-operative cardiac surgery patients gave us the opportunity to control heart rate, since all patients undergoing open-heart surgery are equipped with temporary pacing wires. In the case of aortic valve replacement (AVR) procedures, patients receive not only ventricular but also atrial pacing wires, enabling atrial demand pacing (AAI), a pacing more similar to normal physiology [83]. Thus, throughout the protocols for papers I–III, all patients were subject to AAI pacing in order to keep HR constant.

3.1.1 Study designs

For paper I, we conducted a single-armed prospective study of three sequential interventions with conditions at baseline serving as control. Papers II and III present different data from the same double-armed and double-blind, randomized, controlled trial.

3.1.2 Inclusion, exclusion, randomization, and blinding

Assessing the patients was done prior to surgery on the day of admission. All patients were informed and asked for consent (both oral and written) by one of the investigators. Eligible patients were those scheduled for elective AVR due to AS, and prerequisites were normal LV ejection fraction (>50%) and sinus rhythm on admission. Any co-existing valve disease would exclude the patient, as would any case where a coronary artery disease was the primary indication for the operation. Further, any peri-operative complication would lead to exclusion.

All included patients were randomized to either levosimendan or milrinone at the start of the study. Thus, all patients were included in the data for papers II and III; most patients were also included in the protocol for paper I; but in some cases, the paper I protocol was omitted. The reason for omission was in all these cases due to logistic factors; since most patients were operated in the morning and following a fast track concept, they were supposed to be extubated and leave the intensive care unit before the second case arrived. If this was not possible, we omitted the paper I protocol.

Randomization was performed via closed envelopes and the drugs were prepared by a nurse not involved in the study. This same nurse blinded the infusions and infusion lines to all involved in the study. Also, for blinding reasons, a slight adjustment of the milrinone doses from the standard doses used in clinical settings was made, resulting in equal infusion rates (mL/min) of both drugs at both dose levels.

3.1.3 Experimental protocol

We can regard the protocols for paper I and paper II–III as distinct and separate. This is also how they are referred to in the published papers. However, since many patients followed both protocols sequentially, for ease of reading, they will be described collectively in this thesis.

Prior to surgery, all patients received standard monitoring equipment, including a radial and/or femoral artery catheter, a central venous line, and a trans-esophageal

ultrasound probe. In excess of this, patients had a Swan-Ganz thermodilution catheter placed in the pulmonary artery for right heart catheterization (RHC) data.

Starting in the immediate post-operative period, as soon as the patient was considered hemodynamically stable, randomization was done. Thereafter, two baseline measurements were collected—the calculated means from these were the control values for the first intervention.

Three physiological and two pharmacological interventions followed. After each intervention, all physiologic parameters were allowed to return back to baseline. In this way, all interventions were preceded by a baseline reference point (Fig. 10).

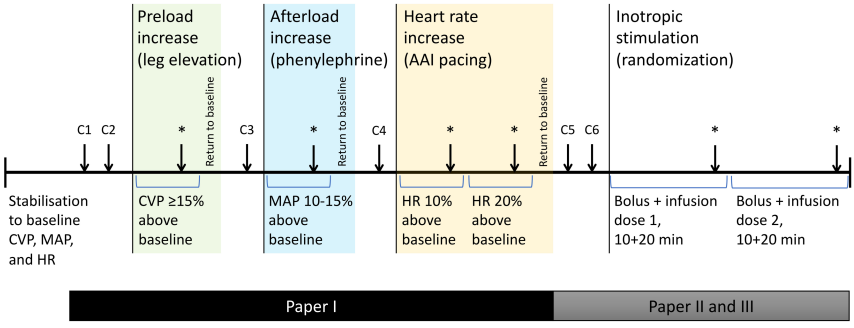

Figure 10. *Combined study protocol for papers I–III*
Each arrow indicates a measurement point. At each point, hemodynamic (RHC) and echocardiographic data are simultaneously collected. C1 *through* C6 *denotes control measurements at baseline levels before interventions (changes in CVP, MAP, and HR). Arrows marked with asterisks (*) are the respective intervention measurements. The baselines for each intervention being: the mean of* C1 *and* C2 *for preload elevation;* C3 *for afterload increase;* C4 *for the two pacing levels; and the mean of* C5 *and* C6 *for the two drug doses. See text for further details.*

3.1.4 Interventions

Already at the start of the study, AAI pacing was commenced on all patients, about 10% above their own sinus rhythm frequency, in order to maintain a controlled HR during the entire protocol. Whenever necessary, to keep a constant CVP (preload), an infusion of colloid was started, and likewise an infusion of phenylephrine to keep a constant MAP (afterload), if needed.

The first physiological intervention was increasing preload through passive leg elevation [84]. Both legs were raised 60° from the supine position with the position of the trunk unchanged. CVP was monitored and when stabilized at a level at least 15% above baseline, measurements were made.

Legs were then lowered and after returning to baseline CVP and yet again having gathered control data, the second intervention followed: increasing afterload. We achieved this by starting or increasing the phenylephrine infusion, adjusting the dose until MAP was at least 10–15% above baseline. Simultaneously, the maximum accepted SAP was decided to 160 mmHg, due to recent surgery.

After the infusion was stopped and baseline conditions restored, a new control measurement was made prior to the third intervention. This was a two-step increase in HR by AAI pacing to 10% and 20% above baseline, with measurements at each frequency.

Finally, after collecting two last control measurements at baseline HR, infusion of the drug started, according to randomization. The drugs were administered in two subsequent doses with measurements after each—both doses starting with a bolus for 10 minutes followed by a 20 minutes infusion. Levosimendan was given at recommended clinical doses of 0.1 and 0.2 μg/kg/min, with boluses of 12 μg/kg. Milrinone was slightly adjusted from its standard doses (for blinding purposes) and given at doses of 0.4 and 0.8 μg/kg/min, with boluses of 50 μg/kg.

3.2 Paper IV

While the preceding papers are all prospective, paper IV is a retrospective cohort study. Patients that had undergone RHC at our hospital during the last two-year period were assessed and only those undergoing a heart transplant or chronic heart failure work-up were included. Another pre-requisite was that echocardiography had been performed within 48 hours of the RHC. Patients with short disease duration and with diseases also affecting the RV, i.e. myocarditis, amyloidosis, and sarcoidosis, as well as any major congenital heart disease and any ventricular assist device, were excluded.

The study was blinded in a way that one investigator did all hemodynamic and LV measurements, while another performed the echocardiographic measurements on the RV. After collecting all hemodynamic (RHC) and echocardiographic data, the patients were divided into three groups:

A. Group A containing patients with normal RV and LV function, defined as a normal right atrial pressure (RAP; <10 mmHg) and normal stroke volume index (SVI; ≥35 mL/m^2);
B. Group B containing patients with normal RAP and reduced SVI (<35 mL/m^2); and finally
C. Group C containing patients with RV failure (RVF), defined by increased RAP (≥10 mmHg).

Data for RAP and SVI were both taken from hemodynamic measurements collected during RHC (Subchapter 3.3).

The three groups were compared for overall and between-group significance in several RV dimensional and functional echocardiographic measurements. A novel RV failure score was then introduced and tested in the same way (Paragraph 3.4.3).

3.3 Hemodynamic measurements

Systemic arterial pressures were all measured invasively by a radial or femoral artery catheter and are referred to as systolic, mean, and diastolic arterial pressures; SAP, MAP, and DAP, respectively.

For central hemodynamics, a pulmonary artery catheter (PAC) was placed through the right internal jugular vein and advanced into either the right or left pulmonary artery by fluoroscopic or pressure guidance. In all four papers, by thermodilution technology, CO was obtained as the mean of three thermodilution measurements [85, 86]. SV was then calculated as SV = CO/HR and further indexed to body surface area (BSA) as stroke volume index (SVI), i.e. SV/BSA. For papers I–III, the PAC was placed prior to surgery.

Via the PAC, diastolic (DPAP), mean (MPAP), and systolic (SPAP) pulmonary artery pressures were measured in addition to RAP, CVP and PCWP, the latter obtained by occlusion of the pulmonary artery by the balloon-tip of the PAC. PCWP was thus not continuously recorded, as CVP, but measured intermittently.

From the above measurements, several parameters were derived. Systemic vascular resistance (SVR) was calculated as SVR = (MAP – CVP)/CO and pulmonary vascular resistance (PVR) as PVR = (MPAP – PCWP)/CO. Pulmonary effective arterial elastance (E_{pa}) was calculated in paper III as E_{pa} = (MPAP – PCWP)/SVI. For paper IV, E_{pa} was *not* indexed and derived from SV instead of SVI. Similarly, SVR and PVR were indexed to BSA in papers II and III (but not in papers I and IV), yielding systemic vascular resistance index (SVRI) and pulmonary vascular resistance index (PVRI), respectively. Note that in paper I-III, the unit used for SVR and PVR is dyn × s/cm^5, while in paper IV we used Wood units (WU). The relation between them is: 1 WU = 80 (dyn × s/cm^5).

Finally, right ventricular stroke work index (RVSWI) was calculated in paper III according to the formula $a \times SVI \times (MPAP - CVP)$. The constant a = 0.0136 g/ml is the Mercury factor, used for converting mmHg of pressure to the unit for work, g × m. RVSWI is the work required to move one SV through the pulmonary vascular system, an integration of stroke volume and systolic pressure load (i.e. afterload minus preload).

3.4 Echocardiographic measurements

A transesophageal echocardiography (TEE) probe, being part of the standard care in cardiac surgery, was inserted at the start of anesthesia in all patients in papers I–III. This probe was kept in place post-operatively for use in our studies. The data in paper IV was obtained from transthoracic echocardiography (TTE) recordings. All echocardiographic measurements were made offline on a workstation using the GE Medical Systems software EchoPAC™.

Deformation imaging by STE (paragraph 1.2.2) was performed in all four studies. In those concerning LV function (papers I and II), longitudinal strain and SR was recorded from the LV inferior wall in the mid-esophageal two-chamber view (ME 2CH). For data on the RV, only the free wall was examined—in paper III via the mid-esophageal four-chamber view (ME 4CH), and in paper IV via a standard, focused or modified apical four-chamber view (A4C). Throughout the protocol for papers I–III, great care was taken keeping the TEE probe unmanipulated so that the exact same part of the respective walls was visualized at all measurement points. All deformation data presented in this thesis was calculated as the mean of three heart cycles and of all three respective segments in each wall, i.e. basal, mid, and apical (Fig. 11).

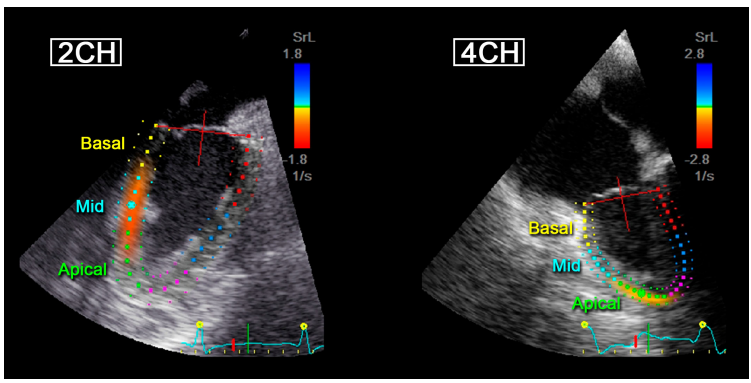

Figure 11. *Wall segments used in deformation imaging*
Left panel showing the three segments of the LV inferior wall in ME 2CH view. Right panel showing the three segments of the RV free wall in ME 4CH view. The means of all three segments was calculated as the LV inferior and RV free wall strain and SR, respectively.

Additionally, in paper III, TAPSE was recorded from the lateral tricuspid annulus in ME 4CH. In paper IV, parameters of longitudinal RV function (TAPSE, TV S', IVV, IVA) were measured from the A4C (see Paragraph 1.3.2 and Fig. 8).

Several dimensional measurements of the RV were used in paper IV (see Paragraph 1.3.1 and Fig. 12): RVOT prox measured in the parasternal long axis view, and RVD1, RVD3, RV EDA, and FAC from the A4C. Two RV transversal dimeters, RV SAX and RV sept, were measured in the parasternal short axis view, and the ratio RV SAX/RV sept used as an index of sphericity. Right and left atrial areas were traced in the A4C, and then indexed to BSA yielding RAAI and LAAI, respectively.

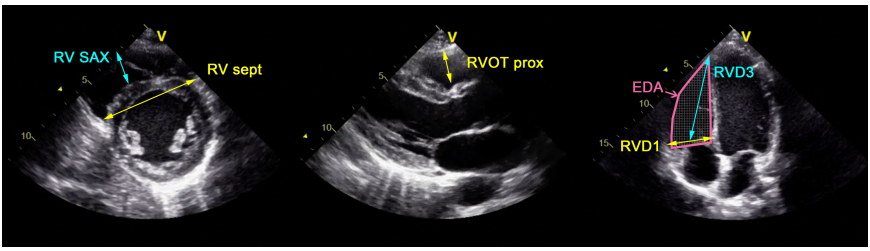

Figure 12. *Right ventricular dimensions*
Left panel: parasternal short axis view with RV sept in yellow and RV SAX in cyan.
Middle panel: parasternal long axis view with RVOT prox diameter.
Right panel: A4C view with RVD1 in yellow, RVD3 in cyan, and an RV EDA trace in magenta.
All measurements performed in end-diastole.

3.4.1 Sphericity index

Potapov et al. introduced a sphericity index that accounts for RV geometry, the idea being that with increasing afterload, a dysfunctional RV will dilate into a more spherical shape, while a RV with preserved contractility will keep its elongated form. In the original paper by Potapov et al., sphericity was defined as the (end-diastolic) short/long axis ratio [87]. In paper IV, we calculated the index by two different ratios: RVD1/RVD3, which is the original ratio described in Potapovs paper, but also RV SAX/RV sept.

A related index is the relation between RV end-diastolic area and long axis, the RV EDA/RVD3 ratio, which we also included. This relation was further evolved by Dandel et al. into the RV loading adaptation index.

3.4.2 RV loading adaptation index

The idea of a healthy RV being able to adapt to increasing afterload in progressive LV failure, led to a proposition by Dandel et al. to relate RV systolic pressure to the sphericity index [88]. A simpler way of obtaining this, however, is to replace pressure

with the velocity time integral of a tricuspid regurgitation jet, the VTI_{TR} (Fig. 13). In this way, they developed the RV loading adaptation index (LAI_{RV}), calculated by the equation:

$$LAI_{RV} = VTI_{TR}/(RV\ EDA/RVD3) = VTI_{TR}(cm) \times RVD3(cm)/RV\ EDA(cm^2)$$

In patients with impaired LV function, a high index indicates a RV adapted to increased afterload, having a high VTI_{TR} with a relatively small RV EDA in relation to RVD3. In other words, the RV has retained its normal shape and size. In this way, the geometry of the RV is considered and integrated with its pressure generating ability.

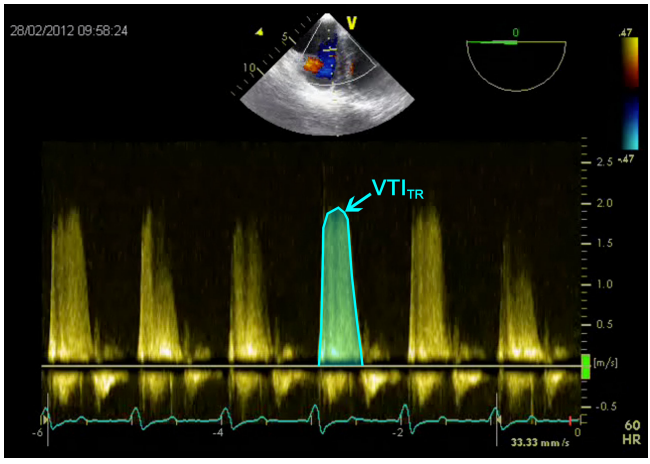

Figure 13. *Velocity time integral*
Continuous Doppler recording of a tricuspid regurgitation jet from the ME 4CH view. The jet is traced and the resulting velocity-time integral (VTI_{TR}) is in cm, as the speed (in cm/s) is multiplied by time (s). This represents the distance that the blood is transported during one heartbeat. The peak velocity of the jet correlates with the systolic pressure gradient (in this case between the RV and the right atrium) through the Bernoulli equation.

3.4.3 Right ventricular failure score

Building upon the idea of RV loading adaptation index, and integrating this with additional RV parameters, we developed a novel score in paper IV, that we call the RV failure score (RVF score).

The score uses six different parameters and we defined cut-off values for each and one. Each parameter that is beyond the cut-off value yields one point, thus the highest possible score is six and the lowest zero.

The parameters and their respective cut-off values were:

1)	RV EDA/BSA	>12 cm^2/m^2
2)	RVD1/RVD3	>0.57
3)	RV free wall strain	> −20%
4)	LAI_{RV}	<14
5)	Estimated CVP (eCVP)	≥10 mmHg
6)	Tricuspid regurgitation	>moderate

In deciding the cut-off values for RV EDA and RV free wall strain, we used normal limits based on population studies and defined in the latest echocardiographic guidelines [44]. CVP was estimated by echocardiography from the collapsibility of the inferior vena cava during inspiration [89] and the cut-off set to 10 mmHg. For the other three parameters, we used the values Dandel et al. showed could identify LVAD patients at risk of developing RV failure [88].

3.5 Statistics

Statistical analyses were performed in SPSS for Macintosh. All values presented are mean ± standard deviation (SD), unless for non-parametric data where instead median ± interquartile range (IQR) is used, or in some instances number and percentage. This is all clearly defined in the tables.

A power analysis was made prior to conducting paper I and II. For the first paper, LV (inferior wall) strain, systolic and diastolic strain rates (SR-S and SR-E) were the primary end-points, while for the second paper, LV strain was the primary end-point. We wanted to detect a 30% change in these parameters. At least 20 patients were needed for paper I versus 15 in each group for papers II and III. As paper III is a secondary analysis, we did a post-hoc power analysis, with the primary endpoint being RV (free wall) strain. In this study we had the power to detect a 20% change in RV strain.

For the first three papers, intra-observer agreement of the deformation analysis was assessed for all parameters (strain, SR-S, and SR-E) by comparing the two initial control measurements, C1 and C2 for paper I, and C5 and C6 for paper II–III (Fig. 10). The coefficient of variation (c_v) was calculated, and we did a Bland-Altman plot to assess the percentage error. The latter is essentially the limit of agreement divided by the mean of both measurements. The formula for percentage error is therefore: $2 \times SD_{diff}/\bar{x}_{a+b}$, where SD_{diff} is the standard deviation of the differences between the measurements, and $\bar{x}_{a+b}$ is the mean of the two measurements [90]. We considered a percentage error of <20% as acceptable, in concordance with studies

on techniques for CO measuring [91]. For c_v (= $SD/\bar{x}$), we accepted a value <10% based on previous studies on deformation [92, 93].

For testing of overall significance between intervention and baseline in paper I, we used a paired t-test for preload and afterload interventions, while for heart rate (having two intervention levels), a two-way analysis of variance (ANOVA) for repeated measurements was used. Whenever overall significance was found, a post-hoc analysis between each heart rate level and baseline was performed using a paired t-test. Sphericity was found in all measurements.

For papers II and III, effects within each intervention group (milrinone or levosimendan) were tested using one-way ANOVA for repeated measurements, followed by a post-hoc analysis as described for paper I. Between-group effects were then analyzed by two-way analysis of co-variance (ANCOVA) for repeated measurements. The ANCOVA was used to adjust for the baseline differences between groups, that unfortunately were encountered, despite randomization, in CO and deformation variables. The mean of the two baseline measurements (C5 and C6) were used as the covariate. Post-hoc testing was performed the same way as in paper I.

In paper IV, for parametric variables, a one-way ANOVA for independent measurements was used in testing overall significance between groups, followed by post-hoc analysis using an independent-samples t-test when appropriate. For non-parametric variables, overall significance was tested using the Kruskal-Wallis test and post-hoc analysis was performed through a Mann-Whitney U test. Categorical data was tested overall with a Pearson Chi^2-test and post-hoc using Fisher's exact test. In all paper IV post-hoc analyses, a Bonferroni correction was made to account for the three groups.

The echocardiographic longitudinal parameters and invasive hemodynamic measurements in paper IV were also assessed for linear relationships using Spearman's correlation coefficient (r).

A p-value of <0.050 was considered significant throughout, except for the Bonferroni corrections in paper IV, where significance was set to p <0.016.

4. Results

Before getting into the published data, some background results that motivated the methodology that we used in paper I–III will be presented. This data is only partly mentioned in the results section of these articles, and the following text will give more details.

4.1 Reproducibility of STE

In the work-up before starting studies I and II, we had seen that intra-observer variability could be significantly reduced if we always kept the TEE probe in the same position, in order to always record the exact same segments of the myocardium at all measurement points. The next step was to investigate which of the projections and LV regions that had the lowest intra-observer variability using speckle tracking echocardiography (STE). We calculated the coefficients of variation between the paired control points (C1 vs C2 and C5 vs C6, respectively) for the LV inferior and anterior walls in ME 2CH, and the interventricular septum and LV lateral wall in ME 4CH. The coefficients of variation (c_v) are presented in Table 2.

Region	Strain	SR-S	SR-E
Inferior wall (ME 2CH)	5.3%	4.4%	6.4%
Anterior wall (ME 2CH)	5.6%	2.4%	10.4%
Septum (ME 4CH)	2.9%	6.4%	5.5%
Lateral wall (ME 4CH)	1.6%	8.2%	13.6%

Table 2. *Coefficients of variation in longitudinal strain and SR by STE from different LV regions*

As we had set our acceptable limit for c_v to <10%, the anterior and lateral walls were excluded from analysis, since SR-E showed too high values. As for the septum, the c_v was adequate for all parameters, but we found a notable drop-out because of poor image quality due to shadowing from the aortic valve prosthesis. The inferior wall was thus chosen for studies I and II as the region of interest for deformation analysis.

Corresponding data for paper III showed the following c_v for STE of the RV free wall: RV strain 4.0%, RV SR-S 5.2% and RV SR-E 5.1%.

4.2 TDI versus STE (unpublished)

Since tissue Doppler imaging (TDI) has a higher frame rate than STE, there is a possibility that we impose a bias using STE, in that STE would yield lower peak values, especially for the strain rates. To address this issue, we compared the methods for their respective c_v, but also for their percentage error and bias (the latter two by Bland-Altman plotting). Recordings from the LV inferior wall at the paired control points C1–C2 were used. The results are presented in Table 3.

Variable	Method	Strain	SR-S	SR-E
Coefficient of variation	TDI	11.9%	10.8%	12.5%
	STE	5.3%	4.4%	6.4%
Percentage error	TDI	38%	36%	63%
	STE	22%	17%	19%
Bias (absolute difference)	STE − TDI	0.94	−0.09	−0.09

Table 3. *Comparing variability and bias for TDI and STE recorded in the LV inferior wall*
Bias was calculated from the absolute values of strain and SR from the two methods. A negative bias in this table means a lower peak SR-S and SR-E derived from STE compared to TDI.

As expected, STE yielded 7.8% lower peak values for SR-S and 12% lower SR-E values relative to TDI. However, the variability (both c_v and Bland-Altman percentage error) in the TDI measurements was almost twice as high compared to STE. For the RV, we did not perform any TDI measurements, since the ME 4CH projection that we used would impose a significant angulation error. Based on the above results, we chose to use only STE for the deformation analysis in paper I–III.

4.3 Paper I

Out of 33 assessed AS patients, 21 were analyzed. Preoperatively, mean aortic valve area was 0.77 cm^2, mean aortic valve gradient 91 mmHg, and mean LV ejection fraction 62%. All patients received a biological aortic valve prosthesis and two had a simultaneous coronary artery by-pass grafting. For further details on exclusions and demographic data, see Paper I.

Preload was increased by passive leg elevation, raising CVP by 29% and PCWP by 20%. This increased CO and SV by 13%, concomitantly with a 9% increase in MAP. All deformation parameters increased significantly (Table 4).

By infusion of phenylephrine at a mean dose of 0.33 μg/kg/min, MAP and SVR increased by 13% and 15%, respectively. CVP was unchanged but PCWP increased

by 10%. Neither SV, nor any of the deformation parameters were significantly affected by afterload increase.

Finally, pacing to 10% and 20% above baseline HR reduced SV incrementally with increased CO (Table 4). No change was seen in LV strain at any pacing level, but the strain rates were affected. LV SR-E increased significantly, starting already at 10% increase, while LV SR-S did not increase until HR was increased by 20%.

Intervention	SV	CO	LV strain	LV SR-S	LV SR-E	PCWP
Preload increase	**13%**	**13%**	**20%**	**11%**	**17%**	**20%**
Afterload increase	*2%*	*0%*	*3%*	*−5%*	*8%*	**10%**
Heart rate increase						
+10%	**−4%**	**5%**	*5%*	*5%*	**19%**	*0%*
+20%	**−13%**	**6%**	*2%*	**7%**	**65%**	*0%*

Table 4. *Effects of increases in load and heart rate on stroke volume and LV deformation*
Significant changes in percent for intervention versus baseline are shown bolded. Numbers in italics denote non-significant changes from baseline.

4.4 Papers II and III

A total of 31 patients were analyzed (out of 42 assessed), whereof 16 in the milrinone group and 15 in the levosimendan group. We had a drop-out of one patient in the levosimendan group in paper II, due to poor visualization of the LV inferior wall. In paper III, two patients in the milrinone group dropped out due to poor visualization of the RV free wall. The same patients were used for both papers and the demographic variables did not differ between groups except for diabetes, that occurred in five levosimendan patients but none in the milrinone group.

Both drugs caused dose-dependent increases in CI and SVI and decreases in SVRI, MAP, and DAP with no differences between groups.

All LV deformation parameters increased dose-dependently with both agents with no differences between groups (Tables 5–7). At the lower dose of milrinone (0.4 μg/kg/min), 85-88% of the maximal response in SVI and LV strain was seen. With levosimendan, the corresponding values were 63-65% at the lower dose (0.1 μg/kg/min). A similar pattern was seen for LV SR-S and SR-E.

For the RV; strain, SR-S, SR-E, and TAPSE all increased dose-dependently with both milrinone and levosimendan with no differences between groups (Table 8).

The phenylephrine doses needed to counteract the drug-induced vasodilation were 0.48 and 0.73 μg/kg/min for milrinone versus 0.30 and 0.51 μg/kg/min for levosimendan at each dose level. The differences between groups were non-significant.

Drug	μg/kg/min	**MAP**	**DAP**	**SPAP**	**MPAP**	**DPAP**
Milrinone	0.40	**−5%**	**−5%**	*10%*	*5%*	*7%*
	0.80	**−5%**	**−5%**	*10%*	*5%*	*7%*
Levosimendan	0.10	*−1%*	*−2%*	**10%**	*5%*	*0%*
	0.20	*−3%*	*−3%*	**10%**	*5%*	*0%*
Between-group *p*		0.786	0.611	0.518	0.061	0.140

Table 5. *Effects of milrinone and levosimendan on systemic and pulmonary pressures*
Significant changes in percent for intervention versus baseline are shown bolded. Numbers in italics denote non-significant changes from baseline.

Drug	μg/kg/min	**CI**	**SVI**	**SVRI**	**PVRI**	**E_{pa}**
Milrinone	0.40	**17%**	**17%**	**−19%**	*−5%*	*−6%*
	0.80	**22%**	**20%**	**−22%**	*−10%*	*−9%*
Levosimendan	0.10	**11%**	**12%**	**−12%**	*−4%*	*−5%*
	0.20	**19%**	**19%**	**−18%**	*−8%*	*−7%*
Between-group *p*		0.744	0.792	0.092	0.321	0.162

Table 6. *Effects of milrinone and levosimendan on CI, SVI, and systemic and pulmonary resistances*
Significant changes in percent for intervention versus baseline are shown bolded. Numbers in italics denote non-significant changes from baseline.

Drug	μg/kg/min	**LV strain**	**LV SR-S**	**LV SR-E**
Milrinone	0.40	**16%**	**17%**	**27%**
	0.80	**18%**	**33%**	**30%**
Levosimendan	0.10	**11%**	**10%**	**13%**
	0.20	**17%**	**23%**	**31%**
Between-group *p*		0.702	0.469	0.637

Table 7. *Effects of milrinone and levosimendan on LV deformation (paper II)*
Significant changes in percent for intervention versus baseline are shown bolded. Numbers in italics denote non-significant changes from baseline.

Drug	μg/kg/min	**RV strain**	**RV SR-S**	**RV SR-E**	**TAPSE**
Milrinone	0.40	**8%**	**8%**	**14%**	**13%**
	0.80	**19%**	**19%**	**24%**	**23%**
Levosimendan	0.10	**10%**	**6%**	**15%**	**11%**
	0.20	**15%**	**20%**	**21%**	**20%**
Between-group *p*		0.259	0.742	0.714	0.742

Table 8. *Effects of milrinone and levosimendan on RV deformation (paper III)*
Significant changes in percent for intervention versus baseline are shown bolded. Numbers in italics denote non-significant changes from baseline.

4.5 Paper IV

From our RHC register, 92 patients were assessed and 68 of these enrolled. The most common diagnosis was dilated cardiomyopathy (53%). From group A to C we saw increasing severity of heart failure when combining ergospirometry data, New York Heart Association (NYHA) class, serum bilirubin, and NT-proBNP levels. Mean LV ejection fraction was 27%, 26%, and 30% in group A, B, and C, respectively. For more details on baseline data, see Table 2 in paper IV.

As RAP and SVI (from RHC) served as grouping parameters, they differed accordingly. All patients with RAP ≥10 mmHg were assigned to group C (n = 22). Those with normal RAP were divided based on their SVI, so that patients with SVI <35 mL/m^2 were referred to group B (n = 21), and those with SVI ≥35 mL/m^2 to group A (n = 25). The means and ranges for RAP and SVI in each group are presented in Table 9. Six patients (27%) in group C had a normal SVI (≥35 mL/m^2).

Variable	Group A	Group B	Group C
RAP	3.6 (0–8)	4.6 (0–9)	13.6 (10–23)
SVI	44 (36–61)	28 (16–34)	31 (18–50)

Table 9. *Distribution of the grouping parameters RAP and SVI in each group*
Values are mean and (range, min–max).

Hemodynamic variables showed that PCWP increased progressively from group A to C, secondary to LV backward failure. PVR was higher in group C compared to group B, while E_{pa} was higher in group C compared to group A (Fig. 14). RVSWI was lower in group B compared to A but showed no significant difference between groups B and C.

Our primary end-point was to find parameters that could distinguish between group B (seemingly normal RV function in the presence of reduced LV function) and group C (reduced RV function). Using a one-way ANOVA for independent measurements, all echocardiographic variables except RVD1/RVD3 and TV S', showed overall significance (p <0.05) between groups. In the subsequent post-hoc analysis, RV longitudinal functional parameters (TAPSE, RV strain, RV SR-S and RV FAC)—with the notable exception of IVV—failed to distinguish between group B and C. On the other hand, all dimensional parameters, except for RV sept, showed significant difference between group B and C. For LAI_{RV}, overall p was 0.045, but subsequent post-hoc analysis revealed no significance between any of the groups.

In Table 10, only echocardiographic variables showing overall significance are presented with their respective post-hoc p-values (significance at p <0.016 due to Bonferroni correction).

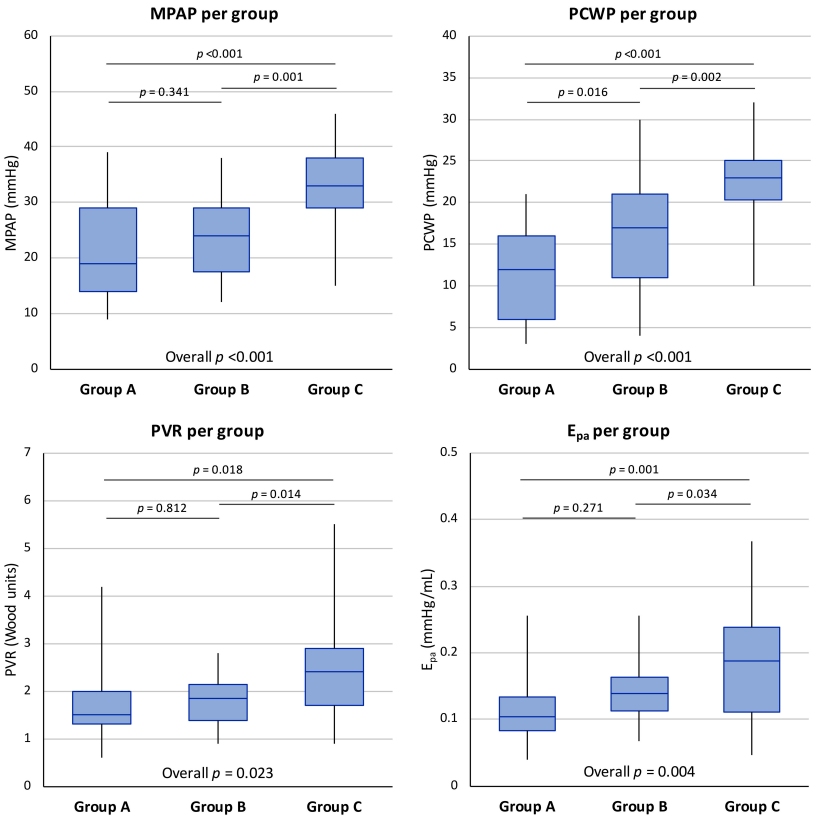

Figure 14. *Amount of LV backward failure and RV impedance in each of the paper IV groups Overall p-value at the bottom of each panel (significance set to <0.050). Between group post-hoc p-values are shown (with Bonferroni correction, significance is set to <0.016).*

Whilst finding cut-off values for the RVF score that we introduced, we found that if RV EDA was indexed to BSA, an index of >12 cm^2/m^2 would differentiate group B from C ($p = 0.002$) on its own, and a more than moderate tricuspid regurgitation would do the same ($p = 0.004$) (Table 10). However, the guideline-recommended cut-off for RV strain (> −20%), as well as the cut-offs proposed by Dandel et al. for LAI_{RV} (<14) and RVD1/RVD3 (>0.57) were non-significant when used in isolation to distinguish group B and C. Integrating these five parameters with echocardiographic-estimated CVP (cut-off ≥10 mmHg), we found that the resulting RVF score was highly significant in distinguishing group B from group C, whereas it showed no difference between groups A and B (overall p <0.001). RVF score results are presented in Table 11 (and paper IV, Fig. 2).

Variable	Group A vs B	Group B vs C	Group A vs C
RV/right atrial dimensions			
RVOT prox	-	0.005	<0.001
RVD1	-	0.004	<0.001
RV EDA	-	0.004	0.002
RV EDA/BSA	-	0.001	0.003
RV EDA/BSA >12 cm^2/m^2	-	0.002	0.002
RV SAX	-	<0.001	<0.001
RV sept	-	-	0.007
RAAI	-	<0.001	<0.001
RAAI >11 cm^2/m^2	-	0.012	0.003
RV geometry			
RV SAX/RV sept	-	<0.001	0.001
RV EDA/RVD3	-	0.005	0.006
RV function			
Grade 3 tricuspid regurgitation	-	0.004	0.004
TAPSE	<0.001	-	<0.001
TAPSE <17 mm	0.002	-	0.002
RV strain	0.008	-	<0.001
RV strain > −20%	-	-	0.003
RV SR-S	-	-	0.009
RV FAC	0.002	-	0.001
RV FAC <35%	0.007	-	0.001
IVV	-	0.009	0.002

Table 10. *Echocardiographic variables from paper IV that showed overall p <0.05*
Between group p-values (p <0.016 significant) are shown. A hyphen indicates non-significance.

RVF score	**Group A**	**Group B**	**Group C**
Median (IQR, 25%–75%)	1 (0–2)	2 (1–2)	4 (3–5)
Post hoc	**Group A vs B**	**Group B vs C**	**Group A vs C**
p-value	0.049	<0.001	<0.001

Table 11. *Right ventricular failure score per group (paper IV)*
Absolute values are median and IQR. Post-hoc p-values are shown. Overall p <0.001.

4.6 RV response to preload and HR (unpublished)

For the sake of completeness, we have also gathered data on the RV effects of isolated increases in preload and heart rate, corresponding to the data from the LV presented in paper I. The measurements were made simultaneously during the experimental procedure for paper I, and performed on the RV free wall in the ME 4CH view. The effects of increasing RV afterload on RV longitudinal function were not assessed, as the increases in SPAP, MPAP, and PVR induced by phenylephrine infusion were low (8%) and considered too minor for any meaningful influence on RV strain or SR. The data presented here is unpublished.

Out of the 21 patients included in paper I, 17 had sufficient visualization of the RV free wall to be included in the STE analysis. Hemodynamic data relevant for the RV was collected from all 21 patients.

Through passive leg elevation, CVP was raised by 29%. Increases in SV and CO were identical to those presented in paper I (+13%). As a result of increased SV and PCWP (the latter by 20%), pulmonary artery pressures increased, SPAP by 13% (p <0.001), MPAP by 12% (p <0.001), and DPAP by 9% (p = 0.001). PVR and pulmonary arterial elastance (measured as E_{pa}) were unaffected. In contrast to the LV, we saw no increase in RV SR-E (p = 0.064), but both RV strain (p = 0.020) and RV SR-S (p = 0.041) increased accordingly, by 11% and 8%, respectively.

By pacing to 10% and 20% above baseline, the effects on SV and CO were equivalent to paper I (SV decreased incrementally with a concomitant increase in CO), with no effect on CVP and PCWP. Pacing did not affect SPAP, while MPAP increased incrementally, by 3% and 5% (overall p = 0.001), and DPAP by 6% at the higher pacing level only (overall p = 0.040). PVR was unaffected, while pulmonary E_{pa} increased by 9% and 25%, respectively (overall p <0.001). Equivalent to the LV, RV SR-E increased significantly by 16% and 51%, respectively (overall p <0.001), and RV SR-S by 17% at the higher pacing level only (overall p = 0.026). Similarly, RV strain was unaffected by increases in HR. Mean ± SD for the RV hemodynamic measurements and STE analyses are presented in Tables 12 and 13, along with the respective significance levels (intervention versus baseline).

Variable	Baseline	Increased preload
RV hemodynamics		
HR (bpm)	81 ± 6	82 ± 6
CVP (mmHg)	7 ± 2	9 ± 2§
PCWP (mmHg)	10 ± 3	12 ± 3***
SPAP (mmHg)	29 ± 7	33 ± 7***
MPAP (mmHg)	20 ± 6	22 ± 5***
DPAP (mmHg)	14 ± 5	15 ± 5***
PVR (dyn × s/cm^5)	181 ± 75	168 ± 61
E_{pa} (mmHg/mL)	0.19 ± 0.08	0.17 ± 0.07
RV speckle tracking echocardiography		
RV strain (%)	−20.0 ± 4.2	−22.2 ± 4.6*
RV SR-S (s^{-1})	−1.72 ± 0.48	−1.86 ± 0.56*
RV SR-E (s^{-1})	1.50 ± 0.35	1.69 ± 0.51

Table 12. *Absolute values of RV measurements at baseline and after increased preload*
Values are mean ± SD. Significance level indicated is for intervention versus baseline as:
**, p <0.050; **, p <0.010; ***, p <0.001; §, not applicable (target of intervention).*

Variable	Baseline	Pacing +10%	Pacing +20%
RV hemodynamics			
HR (bpm)	81 ± 6	89 ± 6§	98 ± 6§
CVP (mmHg)	7 ± 2	7 ± 2	7 ± 2
PCWP (mmHg)	10 ± 3	10 ± 3	10 ± 3
SPAP (mmHg)	29 ± 7	29 ± 8	29 ± 8
MPAP (mmHg)	19 ± 6	20 ± 6*	20 ± 6***
DPAP (mmHg)	13 ± 5	13± 5	14 ± 5**
PVR (dyn × s/cm^5)	177 ± 67	175 ± 79	183 ± 74
E_{pa} (mmHg/mL)	0.18 ± 0.08	0.20 ± 0.10**	0.23 ± 0.10***
RV speckle tracking echocardiography			
RV strain (%)	−20.1 ± 3.9	−19.0 ± 3.3	−20.6 ± 5.3
RV SR-S (s^{-1})	−1.73 ± 0.54	−1.68 ± 0.51	−2.02 ± 0.71*
RV SR-E (s^{-1})	1.48 ± 0.48	1.71 ± 0.54*	2.24 ± 0.48***

Table 13. *Absolute values of RV measurements at baseline and after increased HR*
Values are mean ± SD. Significance level indicated is for intervention versus baseline as:
**, p <0.050; **, p <0.010; ***, p <0.001; §, not applicable (target of intervention).*

5. Discussion

The present thesis has tried to demonstrate, that there is an intricate interaction between cardiac loading conditions, heart rate, myocardial contractility, and not least ventricular interdependence, with respect to the function of the heart. All are evolutionary developments, refined during millions of years, with the purpose of always delivering the required oxygen to all organs in every instant. However, this poses several difficulties to any physician who needs to accurately describe ventricular function. Whenever there is a supposed dysfunction, which in essence means a reduced contractility and/or relaxation, quantifying either is not at all as straightforward as it first may seem, as preload, afterload, and heart rate always needs to be considered. In recent years, the development of ventricular mechanical assist devices has stressed this issue further, and the difficulties in predicting RV failure after LVAD implantation is a proof of this complexity. Both papers I and IV deals with the load dependence of echocardiographic parameters, although from slightly different viewpoints. Papers III and IV are unique in the way they evaluate two inodilators under controlled loading conditions and heart rate. To my knowledge, no other studies have so far been able to isolate the effects in the human heart on contractility and relaxation in this way.

Our findings clearly show, that echocardiographic analysis of ventricular function and deformation, both on the right and left sides of the heart, are strongly dependent on the heart's filling (its preload) and the heart rate. We have also shown, that in the presence of LV forward failure, the sole use of echocardiographic RV longitudinal function indices is not sufficient for evaluation of RV function. Because of this, to correctly assess RV function in this situation, a combination of RV dimensions, its geometry, and functional parameters needs to be evaluated. We introduced a score, consisting of six different RV variables (all easily measured by echocardiography), that in our material was capable of identifying and grading RV failure even in the presence of a LV forward failure. Finally—by keeping preload, outflow impedance, and heart rate constant—we could show that the two commonly used inodilators milrinone and levosimendan (for treating myocardial dysfunction), both improved myocardial contractility and relaxation of the right and left ventricles to a similar extent. Additionally, our results suggest that both drugs exerted equal vasodilating effects on both the systemic and pulmonary vascular beds.

5.1 Methodological issues

One can argue that the highly clinical experimental setting in the paper I–III protocol, using strictly selected post-operative aortic stenosis-patients that had undergone open-heart AVR, and additionally was under general anesthesia with propofol, limits its generalizability. This is of course a valid concern, but it can also be viewed as one of its strengths, since the aim was to study direct effects on myocardial contractility and relaxation by isolated changes in loading, heart rate, and inotropic stimulation. This has to be kept in mind, though, when transferring our results to a general population, where many other factors will interfere. For example, the combined inotropic effect and vasodilation that is induced by both milrinone and levosimendan, is in fact the sought-after effect, since SV and CO will increase profoundly by this synergism. The consequence of this dual action, however, is that if the direct inotropic and lusitropic effects of inodilating drugs are to be assessed (or compared) clinically, preload, afterload, and HR needs to be held constant during pharmacological intervention.

From subchapter 4.2 (TDI versus STE) in the results section, arguments for our method of choice for deformation analysis are presented. Speckle tracking echocardiography (STE) versus tissue Doppler (TDI) was thoroughly evaluated in the work-up for this thesis, and we found that STE was superior in repeatability. However, we are aware that STE yields lower peak values of SR-S and SR-E compared to TDI, due to its lower frame rate. A higher STE frame rate automatically results in lower image quality, and the interval recommended in guidelines is therefore 40–80 frames/s [94]. This can be compared to >100 frames/s achievable with TDI. In short, the relatively low frame rate in STE obviously imposes a risk of missing out on SR peaks, since they might appear in an image frame that is not collected. On the other hand, this limitation would affect all patients equally. Furthermore, the intra-observer variabilities in TDI measurements, at 11–12%, were twice those attained from STE.

Another argument that we need to defend is our choice of a specific myocardial region of interest. Recording LV global strain, i.e. the mean strain of all 17 segments in the LV, would more accurately describe ventricular function, especially for patients with regional wall motion abnormalities. Instead, we chose to just include the LV inferior wall, since this approach enabled us to keep the TEE probe locked in one position, thereby recording exactly the same region of interest at every measurement point. We saw that this restriction greatly enhanced repeatability, since even the slightest manipulation of the TEE probe might result in different regions of interest recorded at different times. Additionally, when we analyzed all LV myocardial walls, the inferior wall had the best image quality overall. However, deformation analysis of the RV is a different story. Methodological studies have indicated that the interventricular septum should be omitted, and that RV free wall strain (as we used both for

paper III and IV) is superior to global RV strain in determining RV function [45, 95]. This approach is also included in the most recent guidelines on RV deformation analysis [96], and is interpreted as a result of the septum being shared between both ventricles. In essence, global RV deformation data will be considerably influenced by LV deformation.

Since cardiopulmonary bypass (CPB) has a negative impact on cardiac function, we need to consider that our patients could have a reduced inotropy and lusitropy at inclusion, which is confirmed by our RV data at baseline. Considering the time span for the experimental protocol in paper I–III (around 2.5 hours), some spontaneous improvement in myocardial contractility and diastolic function could therefore occur during the study. In general, the time between weaning from CPB and the first baseline measurements was around two hours. Since we did two baseline measurements, C1–C2 and C5–C6 (Fig. 10 in the Methods chapter), one hour apart, we could evaluate any impact of time and spontaneous resolution of myocardial function during the experimental procedure. A total of 21 patients had measurements at both baselines, and any significant differences at C5–C6 versus C1–C2 were tested using paired t-tests. Results are presented in Table 14. Systemic and pulmonary pressures were only 5–10% higher at the later baseline point, with similar increases in parameters derived from the arterial pressures, like PVR, E_{pa} and the stroke work indices. Apart from an 8.4% increase in LV strain, there were no other signs of improved RV or LV systolic and diastolic function during our limited time span. We thus believe that time is, at most, a minor confounding factor on our results. It is also worth pointing out that every intervention in the protocol was preceded by a control, as illustrated in Fig. 10.

During administration of the inodilators milrinone and levosimendan, we monitored CVP, SAP, and HR to keep these parameters constant, counteracting the vasodilatory effect of the drugs by phenylephrine infusion and plasma volume expansion. We used CVP as a measure of cardiac preload and targeted SAP as a surrogate for LV afterload, or rather as a measure of LV outflow impedance. In a post-hoc analysis, we calculated the changes in effective aortic (E_a) and pulmonary arterial (E_{pa}) elastances during infusion of milrinone and levosimendan. We found that E_a, equal to LV outflow impedance, decreased slightly (10-15%) with both agents (with no difference between groups), while E_{pa} was unaffected (Fig. 15). To compensate for the increased stroke volumes caused by inotropic stimulation, we should have raised SAP above baseline, by increasing the dose of phenylephrine further, in order to keep afterload and outflow impedance constant. The problem with such an approach, on the other hand, would be to know which exact level of SAP that would correspond to an unchanged afterload.

Variable	C1–C2	C5–C6	Difference
HR (bpm)	81 ± 6	82 ± 6	
CI (L/min/m^2)	2.2 ± 0.4	2.3 ± 0.4	
SVI (mL/m^2)	28 ± 5	28 ± 5	
Phenylephrine dose (µg/kg/min)	0 (0–0.063)	0 (0–0.045)	
LV hemodynamics			
PCWP (mmHg)	10 ± 3	10 ± 3	
SAP (mmHg)	122 ± 20	128 ± 20***	5.3%
MAP (mmHg)	77 ± 9	81 ± 9***	5.3%
DAP (mmHg)	59 ± 7	61 ± 7**	3.4%
SVR (dyn × s/cm^5)	1360 ± 342	1406 ± 389	
LVSWI (g × m/m^2)	25 ± 6	27 ± 7**	8.8%
RV hemodynamics			
CVP (mmHg)	7.4 ± 1.9	7.0 ± 1.8*	−5.6%
SPAP (mmHg)	29 ± 7	31 ± 7***	8.3%
MPAP (mmHg)	19 ± 6	20 ± 6*	4.8%
DPAP (mmHg)	13 ± 5	14± 5	
PVR (dyn × s/cm^5)	177 ± 67	188 ± 69*	6.5%
E_{pa}, non-indexed (mmHg/mL)	0.18 ± 0.08	0.19 ± 0.08*	7.8%
RVSWI (g × m/m^2)	4.6 ± 2.1	5.2 ± 2.1**	13.1%
STE data			
LV strain (%)	−13.0 ± 3.5	−14.1 ± 4.0*	8.4%
LV SR-S (s^{-1})	−1.10 ± 0.31	−1.13 ± 0.35	
LV SR-E (s^{-1})	0.68 ± 0.24	0.75 ± 0.26	
RV strain (%)	−21.3 ± 4.0	−20.4 ± 4.5	
RV SR-S (s^{-1})	−1.73 ± 0.50	−1.77 ± 0.52	
RV SR-E (s^{-1})	1.64 ± 0.45	1.51 ± 0.41	

Table 14. *Absolute values and differences between baseline measurements over time*
About one hour passed between the two baseline points, where C1–C2 served as controls for the pre-load challenge in paper I and C5–C6 as controls for the randomized trial in papers II and III. Data collected from 21 patients that had recordings at both baseline points.
Values are mean ± SD or median and (IQR, 25%–75%). Only significant differences are presented in the right column. Asterisks denote significance levels at C5–C6 versus C1–C2.
**, p <0.050; **, p <0.010; ***, p <0.001.*

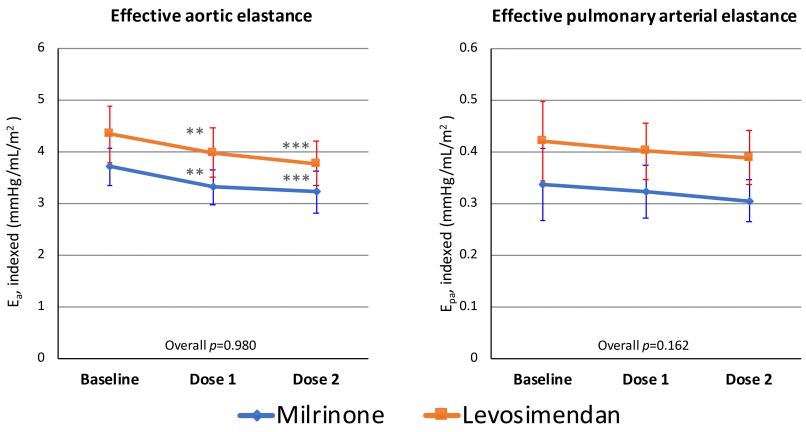

Figure 15. *Effects on effective arterial elastances after inodilator administration*
Data from papers II and III. Left panel showing the systemic (aortic) elastance (E_a) at baseline and after dose 1 and 2 of each drug. Right panel showing the corresponding effects on the pulmonary circulation (E_{pa}). A significant and comparable decrease in E_a was seen with both drugs with no effect on E_{pa}. Overall p is the between-group ANCOVA p-value. Asterisks denote significance at each dose level versus baseline for the respective drug.
**, p <0.050; **, p <0.010; ***, p <0.001.*

From the above, we can conclude that E_a decreased in our material as a consequence of systemic vasodilation, despite the concomitant infusion of a vasopressor. We cannot completely rule out the possibility, that this minor fall (10-15%) in LV outflow impedance during inodilator infusion, could to some extent have affected myocardial deformation. On the other hand, this is less likely, as neither LV strain and SR-S, nor SR-E, seem to be affected by controlled changes in LV outflow impedance, according to the data from paper I.

Finally, for paper IV, one obvious limitation is the retrospective design, as well as the fact that none of the patients were re-assessed at a later state with even more pronounced LV dysfunction. Instead, a total of 43% of patients in the study ended up with a heart transplantation—in contrast to the relatively small number (n = 5) that were later implanted with an LVAD. It is hard to draw any conclusions on this discrepancy, but a larger number of presumptive LVAD patients that could be evaluated for RV failure would give more information on the predictability of the RVF score. A prospective design following patients over time could also better correlate a deteriorating LV function with the RVF score.

5.2 Load and HR effects on myocardial deformation

5.2.1 Effects of preload on myocardial deformation

Raising CVP by 29% and PCWP by 20% resulted in a significant increase in strain, by 20% in the LV and 11% in the RV. This is consistent with the Frank–Starling mechanism [6], as strain is a correlate of SV. Indeed, invasively measured SV and CO increased secondarily. However, we also observed an increase in SR-S in both ventricles, at 8–11%, that would suggest an increased contractility. Furthermore, we saw that LV SR-E increased, suggesting that higher preload will have a positive lusitropic effect as well, at least on the LV.

Only a few previous studies have evaluated the effects of isolated preload changes on cardiac deformation in humans, and the results are contradictory. Recently, Nafati et al. evaluated critically ill patients in a hypovolemic state before and after fluid resuscitation, and they found significant increases in LV strain and SR-S with increasing preload [97]. This is in line with our findings, where patients with LV hypertrophy, secondary to AS, were evaluated. A common denominator in both the study by Nafati et al. and in this thesis, could be a preload dependency among the patients at baseline.

However, other studies on preload and deformation have shown opposing results. In two studies, the effects upon *reduced* preload were assessed. Abali et al. showed that blood donation in healthy volunteers resulted in decreased LV strain, yet with preserved SR-S [24]; while Mendes et al. saw decreased LV SR-E with preserved LV strain and increased SR-S after hemodialysis [25]. Two further studies used nitroglycerin for preload reduction followed by fluid loading or passive leg elevation for preload increase. In the first, by Burns et al., reduced preload resulted in increased LV strain and SR-S, while raising preload instead reduced LV SR-S with no effect on LV strain [27]. On the contrary, Andersen et al. saw no effect at all on LV strain by neither preload increase or decrease [23].

One explanation for this discrepancy, both within these previous studies, as well as compared to our results, might be that awake patients could attenuate or even reverse any preload-induced effect on deformation and CO by an intact baroreceptor response, affecting the sympathetic nervous system output. We discuss this in detail in paper I. For instance, decreasing preload through vasodilation with nitroglycerin, would increase sympathetic output, having a positive inotropic effect, thus increasing LV strain and SR-S. A reversed scenario will be at hand in preload increase, which would lead to a reduced sympathetic output. As we had the opportunity of studying patients under propofol anesthesia, which is an agent known to attenuate or even block the baroreceptor response [98], this confounding effect of the sympathetic nervous system on myocardial deformation was probably minimized.

5.2.2 Effects of afterload on myocardial deformation

Perhaps the first, striking finding in this thesis is the apparent absence of a response to afterload increase in paper I. In any event of abruptly increased afterload, the LV should adapt by increasing its contractility through the Anrep effect—the homeometric autoregulation [4, 5]. This would have been recorded as an increase in SR-S (suggestive of increased myocardial contractility), which was not found. However, to my knowledge, the effects of changes in afterload on myocardial deformation variables have previously not been studied in patients or volunteers.

One explanation might be the administration of phenylephrine, used for afterload increase. As we argue in paper I, phenylephrine works as an α-adrenergic agonist, producing vasoconstriction not only in arterioles, but also in the venous system, leading to recruitment of blood from capacitance vessels, centralizing blood volume, thereby increasing RV and LV preload [99, 100]. Supportive of this is the higher PCWP seen during the afterload challenge (paper I, Table 3). This higher preload will increase all deformation parameters equally, explaining why we did not observe a decrease in SV and strain, as an increase in afterload would yield. A simultaneous increase in pre- and afterload would counteract each other, resulting in a net effect of zero.

The choice of phenylephrine to raise SVR in this thesis, rather than norepinephrine, is based on its pharmacological properties, in that acting as a pure α_1-agonist, it will cause arteriolar and venous vasoconstriction without any direct effect on the myocardium. Norepinephrine, possessing both α_1- and β-stimulation, would increase cardiac contractility as well, thus interfere with our aims [101]. Of course, the above-mentioned problem of increased preload upon phenylephrine administration is a disadvantage, but since no other drug exists that produce an isolated effect on just the arteriolar side, without venous effects, the choice of phenylephrine must be considered the best available for our purpose.

5.2.3 Effects of heart rate on myocardial deformation

Finally, increasing HR by pacing increased both SR-S and SR-E. We interpret the 7% increase in SR-S at the higher pacing level (20% above baseline HR), as increased myocardial contractility due to the Bowditch effect [14-16]. Regarding the increase in SR-E, this was even more pronounced at 20–65%, suggesting a significant positive lusitropic effect by increasing HR. In a study by Esfandiari et al., a similar effect was observed, both in patients with normal heart function, but also (and even more pronounced) in patients with heart failure [102]. They found a shortened time constant (τ) of isovolumic relaxation (an invasive index of early diastolic relaxation, i.e. an equivalent of SR-E). Their results are supportive of the increased SR-E that we saw

in paper I, and indicate that increased HR might improve not only contractility, but also cardiac myocyte handling of Ca^{2+} in both systole and diastole.

However, increasing HR would normally lead to a shorter duration of diastole, thereby reducing ventricular filling. A lower preload will then in turn decrease strain and thus SV. The correlation between decreased end-diastolic volume (EDV) and increased heart rate has been shown experimentally [103]. Likewise, in a study using STE in patients subject to atrial pacing, Mak et al. observed a decrease in LV strain with no effect on SR-S at increased HR [104]. The explanation is probably a pacing-related reduction of EDV and preload in their material, counteracting any increase in SR-S. In our protocol, preload was kept unchanged by colloid infusion, keeping EDV constant, which might explain why strain was unaffected by the HR increase. On the contrary, we did however observe a decrease in SV, which is best explained by a shorter time available for both ventricular ejection and filling.

5.2.4 RV effects of preload and heart rate

The simultaneous effects that we observed in the RV during preload and HR interventions were essentially identical to the ones in the LV, apart from the lack of a statistically significant increase ($p = 0.064$) in RV SR-E during the preload challenge. A possible explanation could be that the study was underpowered in this regard.

In summary, we could reject the null hypothesis that ventricular strain, SR-S, and SR-E are independent of preload and heart rate.

5.3 Inodilators and myocardial deformation

As previously stated, there are very few randomized, controlled studies that directly have compared the cardiac effects of milrinone versus levosimendan. Of those that exist [73-78], all have studied highly selected patients after either cardiac surgery or weaning from extracorporeal circulatory support. In general, they have shown a favourable outcome for levosimendan compared to milrinone. None of them, however, have controlled for the vasodilatory or chronotropic effects of the drugs, so any conclusions on their direct inotropic and lusitropic effects cannot be made.

Of course, a significant proportion of the increase in SV and CO that we see after administration of an inodilator, such as milrinone and levosimendan, is a result of reduced ventricular afterload due to arterial vasodilation. In many instances of a hypotensive cardiogenic shock, however, this additional reduction in blood pressure

may not be favorable, let alone deleterious. Adding an adrenergic drug to uphold MAP is then necessary, counteracting the vasodilation—though inevitably this will attenuate the increase in SV and CO that was originally intended. In our work, we sought to evaluate whether the two inodilators differ in their intrinsic myocardial effects, since any difference would be of clinical value, especially in the critically ill setting.

We counteracted the drug-induced decreases in preload and afterload, resulting from venous and arteriolar vasodilation, by infusion of a colloid and phenylephrine, respectively. In this way, the baroreceptor-induced increase in heart rate, that inodilation normally would yield, was attenuated, and HR could be controlled by pacing. By isolating the intrinsic myocardial effects in this way, we observed no difference in any hemodynamic or echocardiographic variable between milrinone and levosimendan, suggesting that both drugs possess equal inotropic and lusitropic effects. The former being well-documented for both drugs [105-110], but data on the latter are more conflicting. Earlier studies on milrinone have shown positive lusitropic effects when given to chronic heart failure patients [107, 111], but later studies on cardiac surgery patients showed either increased [112] or no lusitropic effects [113, 114]. For levosimendan, on the other hand, its lusitropic property has received much more attention, and in almost all studies showed a positive effect, both in chronic heart failure [109, 110] and cardiac surgery patients [67, 115]. For the LV, this is the first randomized trial comparing the effects of milrinone and levosimendan on LV early diastolic function; and only one randomized trial has been published comparing the inotropic and lusitropic effects on the RV [75]. In that study, by Mishra et al., loading conditions and increases in heart rate were not compensated for, so any conclusions on the intrinsic myocardial effects of the drugs cannot be drawn.

Regarding the effects on the RV, both milrinone and levosimendan have been shown (independently) to increase RV performance and reduce its outflow impedance, through pulmonary vasodilation, in several studies [116-119]. Furthermore, in a study on aortic stenosis patients undergoing AVR, the RV inotropic effect of milrinone was found to be even more pronounced than the effect on the LV [120].

Since evaluation of lusitropic changes was one of our aims, we used patients with aortic stenosis, known for having a reduced LV diastolic function. The choice of including only patients with normal or mildly reduced LV ejection fraction is debatable, since we probably would have seen even more pronounced inotropic effects on a population with LV dysfunction. However, when designing the study, we argued that inclusion of patients with LV dysfunction would result in a significant heterogeneity in baseline data. Despite this limitation, we saw pronounced effects of both inodilators on LV contractility, with an increase in longitudinal LV strain of 17–18% and LV systolic SR of 23–33%.

Comparing baseline data from paper III with data from standard populations, we notice that baseline RV free wall longitudinal strain was clearly reduced in our study. Mean RV free wall strain in our material was −19% at baseline, compared to the normal range of −24% to −29%. It is known that RV longitudinal systolic function is impaired after open-heart surgery, and several possible mechanisms have been proposed, such as pericardial opening or inadequate myocardial protection during cardiopulmonary bypass [121]. Contrary to the normal pre-operative LV function that was a prerequisite in paper II, we can therefore establish that most patients in paper III had reduced RV systolic function at the start of the study—with 83% of the cases having a baseline RV strain higher than −24% (i.e. less negative strain). This is worth noting, but hardly a disadvantage for the results. Both drugs increased longitudinal RV free wall strain by 15–19%, and RV free wall systolic SR by 20%.

Diastolic function increased equally with milrinone and levosimendan, both in the RV and LV, supporting the PDE3-inhibiting mechanism that has previously been shown for levosimendan [65, 66]. The increase in early diastolic SR (SR-E) was 30% in the LV, and 21–24% in the RV.

Despite the fact that there were no significant overall differences in any hemodynamic or echocardiographic deformation parameter between the two drugs, there was a tendency in the milrinone group, that CI, SVI, and LV SR-E increased by a greater fraction already at the lower dose (0.40 μg/kg/min), when compared to the additional increase at the higher dose (0.80 μg/kg/min). Out of the total increase in CI, SVI, and LV SR-E; 77%, 85%, and 90%, respectively, occurred already at the lower dose with milrinone (Fig. 16). However, there was no between-group significance at any of the dose levels. For RV data, no such tendency was seen.

Finally, we saw no between-group significance in phenylephrine doses needed to counteract drug-induced systemic vasodilation, suggesting comparable vasodilatory effects of both drugs. Previous studies are inconsistent in this regard. Two randomized studies on patients weaned from extracorporeal life support [76] and CPB [78], showed equal needs for vasopressor support by both drugs. In contrast, de Hert et al., studying patients with LV dysfunction after CPB, showed higher vasopressor levels in the milrinone group [77], while Mishra et al. found the opposite in post-cardiac surgery patients with LV dysfunction and pulmonary hypertension [75].

In conclusion, the null hypothesis that milrinone and levosimendan are comparable in their LV and RV inotropic and lusitropic effects could *not* be rejected.

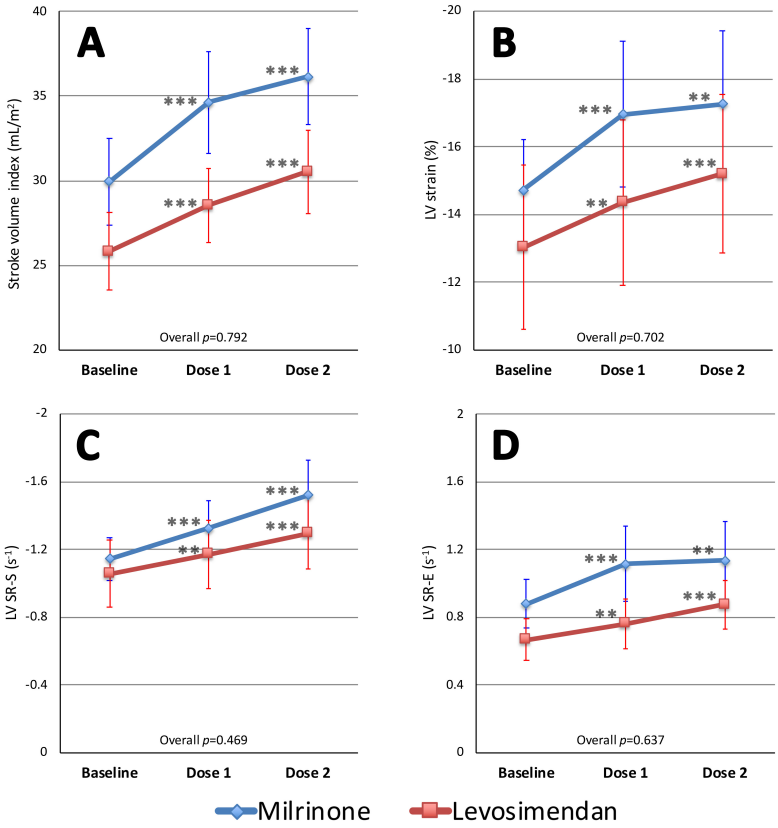

Figure 16. *Plots of SVI and STE data from paper II*
Each panel shows mean and 95% confidence intervals at baseline, dose 1, and dose 2 for milrinone (blue) and levosimendan (red), respectively.
Overall p is the between-group ANCOVA p-value. Asterisks denote significance at each dose level versus baseline for the respective drug.
A tendency towards a pronounced increase already at dose 1 can be seen with milrinone, especially in SVI and LV SR-E. The differences between groups were, however, non-significant.

Panel A: stroke volume index; panel B: LV inferior wall strain; panel C: LV inferior wall systolic strain rate; and panel D: LV inferior wall early diastolic strain rate.

***, p <0.010; ***, p <0.001.*

5.4 Assessment of RV function in left heart disease

5.4.1 General considerations

The last paper is dealing with RV assessment in the presence of LV dysfunction. As we clearly showed in paper I, LV longitudinal deformation measured by echocardiography is affected by changes in preload and heart rate. Thus, reduced deformation does not necessarily indicate reduced contractility, and this is important to acknowledge. To draw any conclusions upon contractility, the confounding factors of preload and heart rate (and probably afterload) need to be controlled. Similar principles apply to the RV, as shown by our unpublished data on RV deformation (Subchapter 4.6 in the Results section). Increased afterload seems to have a relatively greater impact on RV functional parameters than in the LV, yielding lower values with or without any reduction in RV contractility [41, 42, 53]. In a prospective, randomized study on piglets, pulmonary hypertension was induced experimentally, creating an increased RV outflow impedance. This resulted in a reduction in several RV functional parameters (TAPSE, TV S', FAC, and IVA) despite sustained RV contractility [53]. At the same time, it is known that RV function is highly dependent on outflow impedance [41, 42]. So, the question is: can RV echocardiographic parameters of longitudinal function correctly assess the degree of RV functional impairment in a situation with increased RV outflow impedance, such as in LV dysfunction?

In paper IV, we combined a number of echocardiographic variables with invasive data from RHC which, we believe, is a major strength. There are surprisingly few previous studies that have used this approach. In two studies on patients with pulmonary hypertension, RV strain was shown to be dependent on RV outflow impedance, even when contractility was unaffected [122, 123]. In a study on patients with advanced LV failure referred for heart transplant evaluation, RV strain was found to correlate well with invasively defined RV dysfunction, whilst TAPSE and TV S' did not [124]. On the contrary, in a study by Rajagopalan et al., yet again on patients with pulmonary hypertension, RV strain correlated well with RV dysfunction as long as LV function was normal, but in the subgroup of patients that had reduced LV function, no correlation was found between RV strain and RV dysfunction [81]. These findings are in line with what we could show in paper IV.

The difficulties of assessing RV function in LV failure has become a prime focus of echocardiographic research in recent years, as more patients are referred for LVAD implantation. All these patients suffer severe LV dysfunction, but not all of them have reduced RV function. On those that have, implanting an LVAD will increase RV preload and worsen any latent RV dysfunction, creating severe RV failure instead. Identifying patients with latent RV dysfunction is therefore imperative.

Unfortunately, no single echocardiographic measurement of RV longitudinal function has, so far, been shown capable of predicting post-implantation RV failure on its own [80]—a fact that we wanted to address in paper IV.

A retrospective cohort design was set up, where the idea was to compare three groups of patients that had been evaluated both invasively through RHC and with TTE. The grouping of the patients was based on invasive parameters; patients with normal biventricular function were referred to group A, whereas group B had LV dysfunction with normal right atrial pressure (RAP) and decreased SVI, and group C were patients with severely reduced RV function. Defining RV dysfunction is an area of debate, as different studies have used different definitions. We decided that the clinical consequence of RV dysfunction would be that of backward failure, with increased RAP (and CVP). The cut-off most encountered defining RV failure is a RAP ≥10 mmHg, which is the definition of group C. LV dysfunction was defined as SVI <35 mL/m^2, measured by thermodilution during RHC, considered as the gold standard for SV assessment.

The notion that group B patients were working against a higher outflow impedance is not obvious in our data. As shown in Fig. 14 in the results, neither MPAP or PCWP, nor PVR or E_{pa}, showed significant difference between group B to C. Therefore, the reduction in RV longitudinal functional parameters seen in group B might have another explanation. There is a possibility that group B patients in fact had a moderately reduced RV function, but this is debatable. The definition of RV dysfunction is the need for an increased (≥10 mmHg) RAP in order to maintain RV output within the normal range [125]. In order to assess this, the RV reaction to increased RAP, as e.g. by passive leg elevation, would have had to be tested. This data, however, is lacking in our material. Therefore, it is possible that group B patients represent a spectrum of RV function, ranging from normal to moderately reduced.

Individual values of SVI versus RAP are plotted and sorted per group in Fig. 17. Possible Frank–Starling relationship curves are included in the figure with the initial, curved portions derived from non-linear regression analyses of each group's SVI and RAP values. A Frank–Starling curve is a plot relating the SV of a ventricle (in this case the RV) to altering preloads. It is a curvilinear relationship, where the curve will flatten out as the ventricle approaches maximal contractility. Reduced contractility thus produces a more depressed curve. The red line, representing group B, seems to be intermediate to both group A and C, supporting the idea that group B patients could indeed have a moderately reduced RV function.

The null hypothesis was, that echocardiographic measurements of RV longitudinal function would not differ comparing group B and C. The consequence of accepting the null hypothesis is, that whenever LV dysfunction is at hand, changes in RV longitudinal systolic function by echocardiography will not be specific enough for the differentiation between severely and moderately depressed RV function.

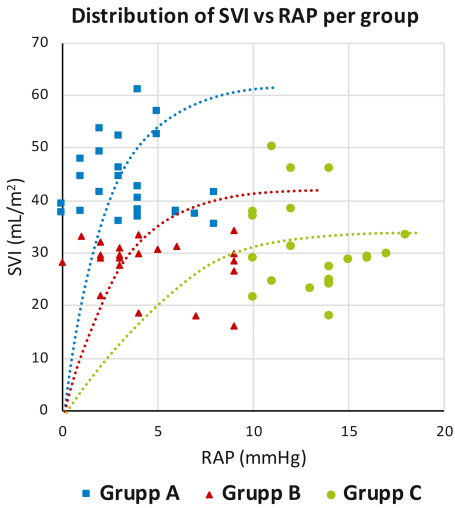

Figure 17. *Scatterplot of individual data from paper IV on SVI and RAP, sorted per group Curves represent possible Frank–Starling relationships for each group and are modified from a non-linear regression analysis.*

5.4.2 Indices of RV sphericity and adaptation to load

Apart from the longitudinal functional parameters, we also assessed measurements of RV dimensions and geometry. Potapov et al. has shown that RV sphericity is a valid measure of RV dysfunction [87]. Their idea is, that a RV exposed to increased outflow impedance can either adapt to the increased load by increased contractility (keeping its normal, elongated shape), or it will dilate and become more spherical. The latter, non-adapted RV will have a high sphericity index, measured as RVD1/RVD3 >0.57, where RVD1 equals the RV short axis and RVD3 its long axis. They found that this parameter alone could identify LVAD patients at risk of developing post-implantation RV failure.

Another measure of RV adaptation, evolved from the sphericity index, is the RV load adaptation index (LAI_{RV}), developed by Dandel et al., integrating RV geometry with its generated systolic pressure (see paragraph 3.4.2) [88]. They found that a value <14 predicted RV failure after LVAD implantation. Unfortunately, in our material, neither the sphericity index, nor LAI_{RV}, could alone distinguish group B from C. A possible reason is revealed when analyzing the generated systolic pressure gradients between the RV and the right atrium (ΔP), which correlates to VTI_{TR}, (a numerator in the LAI_{RV} formula). In Dandel's work, the control group had a ΔP of 42 mmHg compared to 28 mmHg in the RVF group, whereas mean ΔP in

paper IV was 30, 29, and 32 mmHg, respectively for group A–C with no significant difference between groups. This might suggest that even patients in group A could have some degree of RV dysfunction.

However, what Potapov and Dandel showed in their studies were, that RV dimensions and geometry are strongly correlated to RV function, and their conclusions are coherent with the findings in paper IV. All RV dimensional parameters included in our study (except for RV sept) showed significant difference between group B and C. Apart from isovolumic velocity (IVV) and severe tricuspid regurgitation, the functional parameters, on the other hand, showed no significance between group B and C. Furthermore, the relation between longitudinal parameters and invasive RV hemodynamics were weak or non-significant (Table 4 in paper IV).

5.4.3 Clinical implications

The conclusion of this study is consistent with what has been shown both in papers dealing with RV function in patients with pulmonary hypertension or chronic LV failure, as well as those studying outcomes after LVAD. The implication is that echocardiographic indices of RV longitudinal function, such as TAPSE, TV S', FAC, and RV strain, cannot solely be used without taking RV dimensions and geometry into account. The reason has probably to do with the significant load-dependence of the RV, which is much more profound than that of the more muscular LV. On the right side of the circulation, pressures are low, and the RV is not designed for pressure generation. We can look upon the RV as a construction better adapted to variations in flow rather than pressure. Following this line of argument, group B would probably tolerate the increased flow generated by an LVAD better than group C.

Integrating our findings, we developed a score based on a combination of dimensional, geometrical, and functional parameters that we called the right ventricular failure (RVF) score (see paragraph 3.4.3). Our intention was that the score should be strong enough to differentiate severe RV failure (group C) from less pronounced RV dysfunction (group B). It contains six echocardiographic measurements, that are all easy to obtain and thus can be used clinically. We saw that the RVF score indeed showed significant difference between group B and C (p <0.001). Even though RAP was used as a grouping parameter, it could be argued that the inclusion of CVP in the score would be inappropriate and impose a biased result. However, it should be noted that the score contains the non-invasive, estimated CVP from echocardiographic evaluation, denoted as eCVP, and which is not necessarily equal to invasively measured RAP.

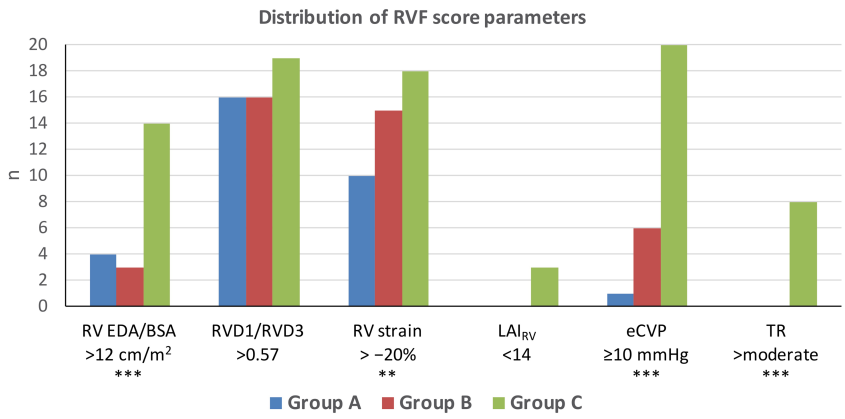

Figure 18. *Distribution of the six RVF score parameters between paper IV groups*
*Diagram showing the number of positive parameters in each group, i.e. with values beyond the cut-off limit for each of the parameters included in the RVF score. TR, tricuspid regurgitation. Asterisks denote overall between-group significance. **, p <0.010; ***, p <0.001.*

In Fig. 18, each of the six RVF score parameters are plotted, separated according to group. Values beyond the cut-off for any of the individual parameters yields one point for that specific parameter, thus n in the figure represents one point in the RVF score. A one-way ANOVA for independent measurements showed overall between-group significance in four of the six parameters: RV EDA/BSA >12 cm/m², RV (free wall) strain > −20%, eCVP ≥10 mmHg, and severe (grade 3) tricuspid regurgitation. The lack of significance for RVD1/RVD3 (RV sphericity index) >0.57 and LAI_{RV} <14 is in concordance with what we saw in the individual assessments of the echocardiographic variables. However, more studies are clearly needed to evaluate the individual contributions of each of the six parameters in a clinical setting, as well as their respective cut-off values.

To summarize, evaluation of RV function by echocardiography needs to consider LV function as well. Whenever a patient with LV dysfunction is assessed, we need to acknowledge that non-invasive measurements of RV longitudinal function cannot be used in isolation for quantifying RV function. Rather, they have to be assessed together with measurements of RV dimensions and geometry, as well as with an estimation of CVP and degree of tricuspid regurgitation. Fortunately, all of this can easily be done by echocardiography.

We could *not* reject the null hypothesis that echocardiographic measurements of longitudinal function were similar between groups B and C.

5.5 Ethical issues

All papers were approved by the University's Institutional Review Board. The retrospective, registry-based paper IV poses few ethical issues. However, the experimental protocol in papers I–III needs some attention.

First, patients included in our study had a pulmonary artery catheter (PAC) inserted prior to surgery. This is not a standard procedure in our department for AVR surgery, and obviously impose an additional risk of complications. For instance, insertion of a PAC can cause local bleeding at the puncture site, including a risk of accidental arterial puncture. Furthermore, the advancement of the PAC through the RV imposes a risk of ventricular arrhythmias. There are also rare cases where the balloon at the catheter's tip have ruptured the pulmonary artery at inflation. Another issue is the time needed for placing the PAC, with subsequent prolongation of the anesthesia time. The latter is only very short in relation to the operation as a whole, and in my opinion negligible. To reduce the risk of vascular complications, all PAC insertions were guided by ultrasound and the internal jugular vein was chosen as the insertion site to reduce the consequences, should a bleeding occur. None of the patients included in the study had any complications from the PAC.

The placement of atrial pacing wires necessary for the study, as well as the insertion of a TEE probe, are both part of standard care for AVR in our department.

A second issue regards the time needed for the study, in total approximately two hours, prolonging anesthesia and mechanical ventilation substantially. However, we saw no adverse effect of this prolongation, and all patients followed standard post-operative care after the protocol was completed.

A third, perhaps more important issue, is the fact that patients included in papers II and III were given an inodilator that they normally would not receive, since their LV function was normal when included. Especially milrinone have been shown to increase the risk of post-operative atrial fibrillation. Furthermore, the vasodilation imposed by both drugs necessitated administration of phenylephrine. The latter, however, carries few risks and was at the time of the study our first-line treatment of CPB-induced vasodilation, meaning that most patients would receive it anyway. Also, we used crystalloid and colloid solutions to compensate for the veno-dilatory effect of the drugs. The mean volumes of these were 1300 mL of Ringer-Acetate® in the levosimendan group and 1500 mL in the milrinone group. This excess volume equals the mean volume that is given in standard care, and has to be seen as a substantial addition. The mean volumes of colloid were more in line with normal post-operative need, ranging from zero up to 300 mL of either albumin or hydroxy-ethyl starch (Voluven®). A few patients received erythrocyte concentrate as part of standard care according to local guidelines.

Finally, we raised SAP during the protocol for paper I, to induce an increase in afterload. Since patients were recently operated upon, we could not increase SAP without accounting for this. Only one patient had to be excluded from the afterload analysis because of this restriction in blood pressure.

All patients were followed up on the first post-operative day and none had any complications.

6. Conclusions

The main findings of the present thesis were:

I. Left (LV) and right (RV) ventricular shortening (strain), as well as velocities of systolic shortening and early diastolic relaxation (strain rates) were all dependent on preload. Neither of these variables were afterload-dependent. Systolic and early diastolic strain rates, but not strain, were affected by changes in heart rate.

II. In the evaluation of the direct effects of various pharmacological interventions on LV and RV contractility and relaxation, studies must be performed at maintained preload, afterload and heart rate.

III. At clinically relevant infusion rates, the direct LV and RV inotropic and lusitropic effects of two commonly used inodilators, milrinone and levosimendan, were comparable when studied at maintained conditions of preload, afterload and heart rate.

IV. In patients with left heart disease, the commonly used RV longitudinal functional variables alone, are not specific enough to detect various degrees of RV dysfunction. Instead, a multi-parametric approach is necessary for correct assessment of RV function, integrating RV dimensions, geometry, load-adaptation, and longitudinal function.

7. Future perspectives

Deformation analysis by speckle tracking echocardiography has been introduced in standard clinical care during the last two decades and strain and strain rate are today firmly integrated in the assessment of cardiac function. The development of this technique is ongoing, and 3-dimensional (3D) imaging is now making its way into clinical practice, where one application receiving much attention is 3D deformation imaging. Especially for the RV, this might be a promising new addition to the arsenal, certainly since the complex 3D shape of the RV makes assessment by 2D echocardiography complicated. Perhaps 3D deformation imaging can prove to be the major breakthrough in assessing RV function? I believe that for the RV, strain and strain rate might become of relatively greater importance than it has proven to be for the LV. Still, it has to be remembered that both strain and strain rate are load dependent, as we have shown, and that this fundamental property of deformation has to be considered even when adding an extra spatial dimension to it.

A natural follow-up study to this thesis would be evaluating milrinone and levosimendan in patients with reduced LV function, using the same protocol as we did in papers II and III. This could be done on patients with reduced LV ejection fraction scheduled for coronary artery bypass grafting, and should be focused primarily on finding differences in inotropic stimulation between the drugs. Still, no other randomized study has compared the two drugs under controlled loading and heart rate.

Further evaluation of the RVF score, as presented in paper IV, is needed, and could be done in several ways. In a retrospective design, LVAD patients could be evaluated in respect to their baseline RVF score before insertion, correlating it with the development of RV failure after implantation. Alternatively, and perhaps more stringent, would be to perform this study using a prospective design, including all patients referred for LVAD evaluation. A problem with the latter approach would be the relatively low frequency of LVAD insertions, which would necessitate a long time-frame, spanning over several years, for patient inclusion. A multi-center study could be an alternative in this respect. Another way to validate the RVF score would be to perform a longitudinal study on RV function, using the RVF score, in patients with LV dysfunction over time. In this way, perhaps more knowledge could be gathered on the progression of RV failure in LV disease, gaining more information on the mechanisms involved.

Acknowledgements

In the making of this thesis, there are many persons that I would like to thank:

First and foremost, professor *Sven-Erik Ricksten*, my supervisor through all these years—always enthusiastic and knowledgeable. Your understanding of physiology is impressive and you are a very good teacher—able to explain the most complicated things in a simple way. Whenever I have needed help, you have always been available and dedicated yourself to the problem without hesitating. Without you, this work would never have been possible, yet even started. Thank you for your patience during all these years!

Kirsten Jørgensen, co-supervisor. It is upon your previous work that this thesis was founded. You guided me through the start-up process and in designing the study. There were many questions in the beginning, that you helped me answer. Many thanks for your support!

Odd Bech-Hanssen, co-author in paper IV. The last paper is, above all, the result of your ideas and curiosity. I have learned a lot from you about echocardiography and you are not just a brilliant clinician, but also a very skilled and thorough researcher. I deeply appreciate all the time you have invested in the design, analyses, results, and conclusions of the last paper. Thank you for your deep engagement in this thesis, even in your spare time!

Erik Houltz, co-author of the first three papers. Thank you for assisting me during the interventions, for your engagement in the inclusion process, and not least for your valuable input on statistics.

My old friend *Mattias Danielson*, present head of the cardiac surgery ward. Your humor and cheerfulness have been a great inspiration. Keep up the good work!

Björn Reinsfelt. Research takes a lot of time from clinical work and needs dedication, not just from those involved, but also from close colleagues. As former head of the cardiac surgery ward, you were always encouraging. No matter how busy you were, you always enabled me to focus on my experiments, even setting time away for deeper questions on statistical problems.

Ulla Nathorst-Westfelt and *Bengt Redfors*, former and present heads of Cardiothoracic anesthesia, and *Helena Rexius*, head of department of Cardiothoracic surgery. Thank you for letting me set aside all this time from clinical work.

Many thanks to *all my colleagues* who have had to put up with my absence from the clinic, and for all your help. You have given me lots of input, not just on practical issues, but also theoretical. Not least all the *surgeons*, who have enabled this work, allowing time and effort in the process.

Thanks to all the *nurses and assistant nurses* that have been involved, both in anesthesia and intensive care. Without you, research would have been much harder, if possible at all. Special thanks to the *coordinators and heads* of the cardiothoracic intensive care unit for your support. Despite logistical inconveniences, I never heard any complaints, and you always found a solution to various problems.

Sven-Erik Bartfay, co-author in paper IV. Thanks for helping me out in the inclusion process and for all aid in the analyses.

Kristjan Karason, co-author in paper IV. Thank you for your valuable input on the manuscript.

Finally, of course, my deepest thanks to my family. For letting me dedicate all this time and never doubting me, for letting me focus in the writing process, and for encouraging me to continue despite moments of doubt. There is a life besides research and work, and without you, it would have been less meaningful.
Thank you, *Marina, Edit and Sixten*!

References

1. Roger S. Seymour, et al., *Evidence for Endothermic Ancestors of Crocodiles at the Stem of Archosaur Evolution.* Physiological and Biochemical Zoology, 2004. **77**(6): p. 1051-1067.

2. Koshiba-Takeuchi, K., et al., *Reptilian heart development and the molecular basis of cardiac chamber evolution.* Nature, 2009. **461**(7260): p. 95-98.

3. Stephenson, A., J. Adams, and M. Vaccarezza, *The vertebrate heart: An evolutionary perspective.* Journal of Anatomy, 2017. **231**.

4. von Anrep, G., *On the part played by the suprarenals in the normal vascular reactions of the body.* The Journal of physiology, 1912. **45**(5): p. 307-317.

5. Cingolani, H., et al., *The Anrep effect: 100 years later*, in *Am. J. Physiol.-Heart Circul. Physiol.* 2013. p. H175-H182.

6. *The Linacre Lecture on the Law of the Heart Given at Cambridge, 1915.* Nature, 1918. **101**(2525): p. 43.

7. Norton, J.M., *TOWARD CONSISTENT DEFINITIONS FOR PRELOAD AND AFTERLOAD.* Advances in Physiology Education, 2001. **25**(1): p. 53-61.

8. Kelly, P.R., et al., *Effective Arterial Elastance as Index of Arterial Vascular Load in Humans.* Circulation, 1992. **86**(2): p. 513-521.

9. Morimont, P., et al., *Effective arterial elastance as an index of pulmonary vascular load.* American Journal of Physiology, 2008. **294**(6): p. H2736.

10. Bernheim, D., *De l'asystolie veineuse dans l'hypertrophie du cœur gauche par sténose concomitante du ventricule droit.* Rev Med, 1910. **39**: p. 785–801.

11. Santamore, W.P., et al., *Ventricular interdependence: Significant left ventricular contributions to right ventricular systolic function.* Progress in Cardiovascular Diseases, 1998. **40**(4): p. 289-308.

12. Naeije, R. and R. Badagliacca, *The overloaded right heart and ventricular interdependence.* Cardiovascular Research, 2017. **113**(12): p. 1474-1485.

13. Damiano, R.J., et al., *Significant left ventricular contribution to right ventricular systolic function.* American Journal of Physiology-Heart and Circulatory Physiology, 1991. **261**(5): p. H1514-H1524.

14. Bowditch, H., *On the peculiarities of excitability which the fibres of cardiac muscle show1, 2.* Leipzig: Physiological Institute, 1871.

15. Piot, C., et al., *High frequency-induced upregulation of human cardiac calcium currents.* Circulation, 1996. **93**(1): p. 120-8.

16. Lakatta, E.G., *Beyond Bowditch: the convergence of cardiac chronotropy and inotropy.* Cell Calcium, 2004. **35**(6): p. 629-42.

17. Suga, A.H., A.K. Sagawa, and A.A. Shoukas, *Load Independence of the Instantaneous Pressure-Volume Ratio of the Canine Left Ventricle and Effects of Epinephrine and Heart Rate on the Ratio.* Circulation Research, 1973. **32**(3): p. 314-322.

18. Kass, D.A., et al., *Use of a conductance (volume) catheter and transient inferior vena caval occlusion for rapid determination of pressure-volume relationships in man.* Cathet Cardiovasc Diagn, 1988. **15**(3): p. 192-202.

19. Sagawa, K., et al., *End-systolic pressure/volume ratio: A new index of ventricular contractility.* The American Journal of Cardiology, 1977. **40**(5): p. 748-753.

20. Gaasch, W.H., et al., *Left ventricular compliance: mechanisms and clinical implications.* The American journal of cardiology, 1976. **38**(5): p. 645.

21. Sutherland, G.R., et al., *Strain and strain rate imaging: a new clinical approach to quantifying regional myocardial function.* Journal of the American Society of Echocardiography, 2004. **17**(7): p. 788-802.

22. Urheim, A.S., et al., *Myocardial Strain by Doppler Echocardiography: Validation of a New Method to Quantify Regional Myocardial Function.* Circulation: Journal of the American Heart Association, 2000. **102**(10): p. 1158-1164.

23. Andersen, N.H., et al., *Influence of preload alterations on parameters of systolic left ventricular long-axis function: A doppler tissue study.* Journal of the American Society of Echocardiography, 2004. **17**(9): p. 941-947.

24. Abali, G., et al., *Which Doppler Parameters Are Load Independent? A Study in Normal Volunteers After Blood Donation.* Journal of the American Society of Echocardiography, 2005. **18**(12): p. 1260-1265.

25. Mendes, L., et al., *Load-independent parameters of diastolic and systolic function by speckle tracking and tissue doppler in hemodialysis patients.* Rev Port Cardiol, 2008. **27**(9): p. 1011-25.

26. Rosner, A., et al., *Left ventricular size determines tissue Doppler-derived longitudinal strain and strain rate.* Eur J Echocardiogr, 2009. **10**(2): p. 271-7.

27. Burns, A.T., et al., *Left ventricular strain and strain rate: characterization of the effect of load in human subjects.* European journal of echocardiography : the journal of the Working Group on Echocardiography of the European Society of Cardiology, 2010. **11**(3): p. 283.

28. A'roch, R., et al., *Left ventricular strain and peak systolic velocity: responses to controlled changes in load and contractility, explored in a porcine model.* Cardiovascular Ultrasound, 2012. **10**(1).

29. Ferferieva, V., et al., *The relative value of strain and strain rate for defining intrinsic myocardial function.* American Journal of Physiology, 2012. **302**(1): p. H188.

30. Dahle, G.O., et al., *The influence of acute unloading on left ventricular strain and strain rate by speckle tracking echocardiography in a porcine model.* American journal of physiology. Heart and circulatory physiology, 2016. **310**(10): p. H1330.

31. Leischik, R., B. Dworrak, and K. Hensel, *Intraobserver and interobserver reproducibility for radial, circumferential and longitudinal strain echocardiography.* Open Cardiovasc Med J, 2014. **8**: p. 102-9.

32. Sugimoto, T., et al., *Echocardiographic reference ranges for normal left ventricular 2D strain: results from the EACVI NORRE study.* European Heart Journal - Cardiovascular Imaging, 2017. **18**(8): p. 833-840.

33. Muraru, P.D., et al., *Sex- and Method-Specific Reference Values for Right Ventricular Strain by 2-Dimensional Speckle-Tracking Echocardiography.* Circulation: Cardiovascular Imaging, 2016. **9**(2): p. e003866-e003866.

34. Langeland, F.S., et al., *Experimental Validation of a New Ultrasound Method for the Simultaneous Assessment of Radial and Longitudinal Myocardial Deformation Independent of Insonation Angle.* Circulation, 2005. **112**(14): p. 2157-2162.

35. Amundsen, B.H., et al., *Regional myocardial long-axis strain and strain rate measured by different tissue Doppler and speckle tracking echocardiography methods: a comparison with tagged magnetic resonance imaging.* European Journal of Echocardiography, 2009. **10**(2): p. 229-237.

36. Bohs, L.N. and G.E. Trahey, *A novel method for angle independent ultrasonic imaging of blood flow and tissue motion.* IEEE Transactions on Biomedical Engineering, 1991. **38**(3): p. 280-286.

37. Abuelkasem, E., et al., *Perioperative clinical utility of myocardial deformation imaging: a narrative review.* Br J Anaesth, 2019. **123**(4): p. 408-420.

38. Takemoto, Y., et al., *Analysis of the Interaction Between Segmental Relaxation Patterns and Global Diastolic Function by Strain Echocardiography.* Journal of the American Society of Echocardiography, 2005. **18**(9): p. 901-906.

39. Støylen, A., et al., *Strain rate imaging in normal and reduced diastolic function: Comparison with pulsed doppler tissue imaging of the mitral annulus.* Journal of the American Society of Echocardiography, 2001. **14**(4): p. 264-274.

40. Walker, L.A. and P.M. Buttrick, *The right ventricle: biologic insights and response to disease.* Current cardiology reviews, 2009. **5**(1): p. 22-28.

41. Bosch, L., et al., *Right ventricular dysfunction in left-sided heart failure with preserved versus reduced ejection fraction.* European Journal of Heart Failure, 2017. **19**(12): p. 1664-1671.

42. Schwarz, K., et al., *Right Ventricular Function in Left Ventricular Disease: Pathophysiology and Implications.* Heart, Lung and Circulation, 2013. **22**(7): p. 507-511.

43. Rudski, L.G., et al., *Guidelines for the Echocardiographic Assessment of the Right Heart in Adults: A Report from the American Society of Echocardiography: Endorsed by the European Association of Echocardiography, a registered branch of the European Society of Cardiology, and the Canadian Society of Echocardiography.* Journal of the American Society of Echocardiography, 2010. **23**(7): p. 685-713.

44. Lang, R.M., et al., *Recommendations for Cardiac Chamber Quantification by Echocardiography in Adults: An Update from the American Society of Echocardiography and the European Association of Cardiovascular Imaging.* Journal of the American Society of Echocardiography, 2015. **28**(1): p. 1-39.e14.

45. Focardi, M., et al., *Traditional and innovative echocardiographic parameters for the analysis of right ventricular performance in comparison with cardiac magnetic resonance.* Eur Heart J Cardiovasc Imaging, 2015. **16**(1): p. 47-52.

46. Kaul, S., et al., *Assessment of right ventricular function using two-dimensional echocardiography.* American Heart Journal, 1984. **107**(3): p. 526-531.

47. Aloia, E., et al., *TAPSE: An old but useful tool in different diseases.* Int J Cardiol, 2016. **225**: p. 177-183.

48. Isaaz, K., et al., *Quantitation of the motion of the cardiac base in normal subjects by Doppler echocardiography.* J Am Soc Echocardiogr, 1993. **6**(2): p. 166-76.

49. Lindqvist, P., et al., *The use of isovolumic contraction velocity to determine right ventricular state of contractility and filling pressures: A pulsed Doppler tissue imaging study.* European Heart Journal - Cardiovascular Imaging, 2005. **6**(4): p. 264-270.

50. Vogel, R.M., et al., *Validation of Myocardial Acceleration During Isovolumic Contraction as a Novel Noninvasive Index of Right Ventricular Contractility: Comparison With Ventricular Pressure-Volume Relations in an Animal Model.* Circulation: Journal of the American Heart Association, 2002. **105**(14): p. 1693-1699.

51. Kind, T., et al., *Right ventricular ejection fraction is better reflected by transverse rather than longitudinal wall motion in pulmonary hypertension.* Journal of Cardiovascular Magnetic Resonance, 2010. **12**(1): p. 35.

52. Mauritz, G.-J., et al., *Progressive Changes in Right Ventricular Geometric Shortening and Long-term Survival in Pulmonary Arterial Hypertension.* Chest, 2012. **141**(4): p. 935-943.

53. Guihaire, J., et al., *Non-invasive indices of right ventricular function are markers of ventricular-arterial coupling rather than ventricular contractility: insights from a porcine model of chronic pressure overload.* Eur Heart J Cardiovasc Imaging, 2013. **14**(12): p. 1140-9.

54. Beavo, J.A. and L.L. Brunton, *Cyclic nucleotide research — still expanding after half a century.* Nature Reviews Molecular Cell Biology, 2002. **3**(9): p. 710-717.

55. Feneck, R., *Phosphodiesterase inhibitors and the cardiovascular system.* BJA Education, 2007. **7**(6): p. 203-207.

56. Alousi, A.A., et al., *Cardiotonic activity of milrinone, a new and potent cardiac bipyridine, on the normal and failing heart of experimental animals.* J Cardiovasc Pharmacol, 1983. **5**(5): p. 792-803.

57. Mager, G., et al., *Phosphodiesterase III inhibition or adrenoreceptor stimulation: milrinone as an alternative to dobutamine in the treatment of severe heart failure.* Am Heart J, 1991. **121**(6 Pt 2): p. 1974-83.

58. Colucci, W.S., et al., *Milrinone and dobutamine in severe heart failure: differing hemodynamic effects and individual patient responsiveness.* Circulation, 1986. **73**(3 Pt 2): p. III175-83.

59. Ponikowski, P., et al., *2016 ESC Guidelines for the diagnosis and treatment of acute and chronic heart failure: The Task Force for the diagnosis and treatment of acute and chronic heart failure of the European Society of Cardiology (ESC)Developed with the special contribution of the Heart Failure Association (HFA) of the ESC.* European Heart Journal, 2016. **37**(27): p. 2129-2200.

60. Yancy, C.W., et al., *2013 ACCF/AHA Guideline for the Management of Heart Failure.* Circulation, 2013. **128**(16): p. e240-e327.

61. Bayram, M., et al., *Reassessment of dobutamine, dopamine, and milrinone in the management of acute heart failure syndromes.* Am J Cardiol, 2005. **96**(6a): p. 47g-58g.

62. Hajjar, R. and J. Gwathmey, *Calcium-sensitizing inotropic agents in the treatment of heart failure: A critical view.* Cardiovascular Drugs and Therapy, 1991. **5**(6): p. 961-965.

63. Pollesello, P., et al., *Binding of a new Ca2+ sensitizer, levosimendan, to recombinant human cardiac troponin C. A molecular modelling, fluorescence probe, and proton nuclear magnetic resonance study.* Journal of Biological Chemistry, 1994. **269**(46): p. 28584-28590.

64. Haikala, H., et al., *Cardiac troponin C as a target protein for a novel calcium sensitizing drug, levosimendan.* J Mol Cell Cardiol, 1995. **27**(9): p. 1859-66.

65. Hasenfuss, G., et al., *Influence of the novel inotropic agent levosimendan on isometric tension and calcium cycling in failing human myocardium.* Circulation, 1998. **98**(20): p. 2141-7.

66. Orstavik, O., et al., *Inhibition of phosphodiesterase-3 by levosimendan is sufficient to account for its inotropic effect in failing human heart.* Br J Pharmacol, 2014. **171**(23): p. 5169-81.

67. Jorgensen, K., et al., *Effects of levosimendan on left ventricular relaxation and early filling at maintained preload and afterload conditions after aortic valve replacement for aortic stenosis.* Circulation, 2008. **117**(8): p. 1075-81.

68. Höhn, J., et al., *Levosimendan Interacts with Potassium Channel Blockers in Human Saphenous Veins.* Basic & Clinical Pharmacology & Toxicology, 2004. **94**(6): p. 271-273.

69. Erdei, N., et al., *The levosimendan metabolite OR-1896 elicits vasodilation by activating the KATP and BKCa channels in rat isolated arterioles.* British Journal of Pharmacology, 2006. **148**(5): p. 696-702.

70. Kivikko, M., et al., *Pharmacokinetics of levosimendan and its metabolites during and after a 24-hour continuous infusion in patients with severe heart failure.* Int J Clin Pharmacol Ther, 2002. **40**(10): p. 465-71.

71. Ukkonen, H., et al., *Myocardial efficiency during levosimendan infusion in congestive heart failure.* Clinical Pharmacology & Therapeutics, 2000. **68**(5): p. 522-531.

72. Landoni, G., et al., *Effects of levosimendan on mortality and hospitalization. A meta-analysis of randomized controlled studies*.* Critical Care Medicine, 2012. **40**(2): p. 634-646.

73. Al-Shawaf, E., et al., *Levosimendan or milrinone in the type 2 diabetic patient with low ejection fraction undergoing elective coronary artery surgery.* J Cardiothorac Vasc Anesth, 2006. **20**(3): p. 353-7.

74. Lechner, E., et al., *Levosimendan versus milrinone in neonates and infants after corrective open-heart surgery: a pilot study.* Pediatr Crit Care Med, 2012. **13**(5): p. 542-8.

75. Mishra, A., et al., *Comparative Effect of Levosimendan and Milrinone in Cardiac Surgery Patients With Pulmonary Hypertension and Left Ventricular Dysfunction.* Journal of Cardiothoracic and Vascular Anesthesia, 2016. **30**(3): p. 639-646.

76. Jacky, A., et al., *Comparison of Levosimendan and Milrinone for ECLS Weaning in Patients After Cardiac Surgery-A Retrospective Before-and-After Study.* J Cardiothorac Vasc Anesth, 2018. **32**(5): p. 2112-2119.

77. De Hert, S.G., et al., *The effects of levosimendan in cardiac surgery patients with poor left ventricular function.* Anesth Analg, 2007. **104**(4): p. 766-73.

78. Sunny, et al., *Comparison of Levosimendan, Milrinone and Dobutamine in treating Low Cardiac Output Syndrome Following Valve Replacement Surgeries with Cardiopulmonary Bypass.* J Clin Diagn Res, 2016. **10**(12): p. Uc05-uc08.

79. Konstam, A.M., et al., *Evaluation and Management of Right-Sided Heart Failure: A Scientific Statement From the American Heart Association.* Circulation, 2018. **137**(20): p. e578-e622.

80. Paluszkiewicz, L. and J. Börgermann, *The value of echocardiographic examination in predicting right ventricular heart failure in patients after the implantation of continuous-flow left ventricular assist devices†.* Interactive CardioVascular and Thoracic Surgery, 2018. **27**(6): p. 931-937.

81. Rajagopalan, N., et al., *Utility of Right Ventricular Tissue Doppler Imaging: Correlation with Right Heart Catheterization.* Echocardiography, 2008. **25**(7): p. 706-711.

82. Kampaktsis, P.N., et al., *The role and clinical implications of diastolic dysfunction in aortic stenosis.* Heart, 2017. **103**(19): p. 1481-1487.

83. Reade, M.C., *Temporary epicardial pacing after cardiac surgery: a practical review.* Anaesthesia, 2007. **62**(4): p. 364-373.

84. Caille, V., et al., *Hemodynamic effects of passive leg raising: an echocardiographic study in patients with shock.* Intensive Care Medicine, 2008. **34**(7): p. 1239-1245.

85. Ganz, W., et al., *A new technique for measurement of cardiac output by thermodilution in man.* The American Journal of Cardiology, 1971. **27**(4): p. 392-396.

86. Opotowsky, A.R., et al., *Thermodilution vs Estimated Fick Cardiac Output Measurement in Clinical Practice: An Analysis of Mortality From the Veterans Affairs Clinical Assessment, Reporting, and Tracking (VA CART) Program and Vanderbilt University.* JAMA Cardiology, 2017. **2**(10): p. 1090-1099.

87. Potapov, E.V., et al., *Tricuspid Incompetence and Geometry of the Right Ventricle as Predictors of Right Ventricular Function After Implantation of a Left Ventricular Assist Device.* Journal of Heart and Lung Transplantation, 2008. **27**(12): p. 1275-1281.

88. Dandel, M., et al., *Load Dependency of Right Ventricular Performance Is a Major Factor to be Considered in Decision Making Before Ventricular Assist Device Implantation.* Circulation, 2013. **128**(11_suppl_1 Suppl 1): p. S14-S23.

89. Kircher, B.J., R.B. Himelman, and N.B. Schiller, *Noninvasive estimation of right atrial pressure from the inspiratory collapse of the inferior vena cava.* The American Journal of Cardiology, 1990. **66**(4): p. 493-496.

90. Hanneman, K.S., *Design, Analysis, and Interpretation of Method-Comparison Studies.* AACN Advanced Critical Care, 2008. **19**(2): p. 223-234.

91. Critchley, L. and J. Critchley, *A Meta-Analysis of Studies Using Bias and Precision Statistics to Compare Cardiac Output Measurement Techniques.* Journal of Clinical Monitoring and Computing, 1999. **15**(2): p. 85-91.

92. Cheng, S., et al., *Reproducibility of speckle-tracking-based strain measures of left ventricular function in a community-based study.* Journal of the American Society of Echocardiography : official publication of the American Society of Echocardiography, 2013. **26**(11): p. 1258-1266.e2.

93. Risum, N., et al., *Variability of Global Left Ventricular Deformation Analysis Using Vendor Dependent and Independent Two-Dimensional Speckle-Tracking Software in Adults.* Journal of the American Society of Echocardiography, 2012. **25**(11): p. 1195-1203.

94. Voigt, J.-U., et al., *Definitions for a common standard for 2D speckle tracking echocardiography: consensus document of the EACVI/ASE/Industry Task Force to standardize deformation imaging.* European Heart Journal – Cardiovascular Imaging, 2015. **16**(1): p. 1.

95. Hamada-Harimura, Y., et al., *Incremental Prognostic Value of Right Ventricular Strain in Patients With Acute Decompensated Heart Failure.* Circulation: Cardiovascular Imaging, 2018. **11**(10): p. e007249.

96. Badano, L.P., et al., *Standardization of left atrial, right ventricular, and right atrial deformation imaging using two-dimensional speckle tracking echocardiography: a consensus document of the EACVI/ASE/Industry Task Force to standardize deformation imaging.* European Heart Journal - Cardiovascular Imaging, 2018. **19**(6): p. 591-600.

97. Nafati, C., et al., *Use of speckle-tracking strain in preload-dependent patients, need for cautious interpretation!* Annals of Intensive Care, 2018. **8**(1): p. 1-8.

98. Sato, M., et al., *Baroreflex control of heart rate during and after propofol infusion in humans.* BJA: British Journal of Anaesthesia, 2005. **94**(5): p. 577-581.

99. Nygren, A., A. Thorén, and S.-E. Ricksten, *Vasopressors and intestinal mucosal perfusion after cardiac surgery: Norepinephrine vs. phenylephrine.* Critical Care Medicine, 2006. **34**(3): p. 722-729.

100. Kalmar, A.F., et al., *Phenylephrine increases cardiac output by raising cardiac preload in patients with anesthesia induced hypotension.* J Clin Monit Comput, 2018. **32**(6): p. 969-976.

101. Mets, B., *Should Norepinephrine, Rather than Phenylephrine, Be Considered the Primary Vasopressor in Anesthetic Practice?* Anesthesia & Analgesia, 2016. **122**(5): p. 1707-1714.

102. Esfandiari, S., et al., *Heart rate–dependent left ventricular diastolic function in patients with and without heart failure.* Journal of cardiac failure, 2015. **21**(1): p. 68-75.

103. Ilebekk, A., et al., *Cardiac performance: optimal heart rate for maximal cardiac output.* Scand J Clin Lab Invest, 1979. **39**(1): p. 79-85.

104. Mak, S., et al., *Strain, strain rate, and the force frequency relationship in patients with and without heart failure.* Journal of the American Society of Echocardiography, 2012. **25**(3): p. 341-348.

105. Borow, K.M., et al., *Physiologic assessment of the inotropic, vasodilator and afterload reducing effects of milrinone in subjects without cardiac disease.* The American Journal of Cardiology, 1985. **55**(9): p. 1204-1209.

106. Jaski, B.E., et al., *Positive inotropic and vasodilator actions of milrinone in patients with severe congestive heart failure. Dose-response relationships and comparison to nitroprusside.* The Journal of clinical investigation, 1985. **75**(2): p. 643.

107. Brecker, S.J., et al., *Effects of intravenous milrinone on left ventricular function in ischemic and idiopathic dilated cardiomyopathy.* Am J Cardiol, 1993. **71**(2): p. 203-9.

108. Sonntag, S., et al., *The calcium sensitizer levosimendan improves the function of stunned myocardium after percutaneous transluminal coronary angioplasty in acute myocardial ischemia.* J Am Coll Cardiol, 2004. **43**(12): p. 2177-82.

109. Givertz, M.M., et al., *Direct myocardial effects of levosimendan in humans with left ventricular dysfunction: alteration of force-frequency and relaxation-frequency relationships.* Circulation, 2007. **115**(10): p. 1218-24.

110. Lunghetti, S., et al., *Effects of levosimendan without loading dose on systolic and diastolic function in patients with end-stage heart failure.* Cardiol J, 2011. **18**(5): p. 532-7.

111. Hadano, Y., et al., *Impact of milrinone on mitral annular velocity in patients with congestive heart failure.* J Med Ultrason (2001), 2013. **40**(2): p. 111-8.

112. Axelsson, B., et al., *Milrinone improves diastolic function in coronary artery bypass surgery as assessed by acoustic quantification and peak filling rate: a prospective randomized study.* J Cardiothorac Vasc Anesth, 2010. **24**(2): p. 244-9.

113. Couture, P., et al., *Milrinone enhances systolic, but not diastolic function during coronary artery bypass grafting surgery.* Can J Anaesth, 2007. **54**(7): p. 509-22.

114. Lobato, E.B., et al., *Effects of milrinone versus epinephrine on left ventricular relaxation after cardiopulmonary bypass following myocardial revascularization: assessment by color m-mode and tissue Doppler.* J Cardiothorac Vasc Anesth, 2005. **19**(3): p. 334-9.

115. Malik, V., et al., *Effect of Levosimendan on Diastolic Function in Patients Undergoing Coronary Artery Bypass Grafting: A Comparative Study.* J Cardiovasc Pharmacol, 2015. **66**(2): p. 141-7.

116. Eichhorn, E.J., et al., *Differential effects of milrinone and dobutamine on right ventricular preload, afterload and systolic performance in congestive heart failure secondary to ischemic or idiopathic dilated cardiomyopathy.* The American Journal of Cardiology, 1987. **60**(16): p. 1329-1333.

117. Yilmaz, M.B., et al., *Comparative effects of levosimendan and dobutamine on right ventricular function in patients with biventricular heart failure.* Heart and Vessels, 2009. **24**(1): p. 16-21.

118. Feneck, R.O., *Intravenous milrinone following cardiac surgery: I. effects of bolus infusion followed by variable dose maintenance infusion.* Journal of Cardiothoracic and Vascular Anesthesia, 1992. **6**(5): p. 554-562.

119. Mansiroglu, A.K., et al., *Assessment of sustained effects of levosimendan on right ventricular systolic functions in patients with advanced heart failure.* Acta Cardiologica, 2016. **71**(4): p. 411-415.

120. Maslow, A.D., et al., *Inotropes improve right heart function in patients undergoing aortic valve replacement for aortic stenosis.* Anesth Analg, 2004. **98**(4): p. 891-902, table of contents.

121. Tamborini, G., et al., *Is right ventricular systolic function reduced after cardiac surgery? A two- and three-dimensional echocardiographic study.* European Journal of Echocardiography, 2009. **10**(5): p. 630-634.

122. Simon, M.A., et al., *Tissue Doppler imaging of right ventricular decompensation in pulmonary hypertension.* Congest Heart Fail, 2009. **15**(6): p. 271-6.

123. Urheim, S., et al., *Relation of tissue displacement and strain to invasively determined right ventricular stroke volume.* Am J Cardiol, 2005. **96**(8): p. 1173-8.

124. Cameli, M., et al., *Right ventricular longitudinal strain correlates well with right ventricular stroke work index in patients with advanced heart failure referred for heart transplantation.* J Card Fail, 2012. **18**(3): p. 208-15.

125. Lang, I.M., *Management of acute and chronic RV dysfunction.* European Heart Journal Supplements, 2007. **9**(suppl_H): p. H61-H67.

Appendices

App. 1. The right ventricular failure (RVF) score

RVF SCORE PARAMETERS	**FORMULA**	**CUT-OFF**	**POINTS (0 or 1)**
RV end-diastolic area index	$\frac{\text{RV EDA}}{\text{BSA}}$	>12 cm²/m²	
RV sphericity index	$\frac{\text{RVD1}}{\text{RVD3}}$	>0.57	
RV free wall longitudinal strain		> −20%	
RV load adaptation index (LAI_{RV})	$\frac{\text{VTI}_{TR} \times \text{RVD3}}{\text{RV EDA}}$	<14	
Estimated CVP		≥10 mmHg	
Tricuspid regurgitation		>moderate	

Each parameter beyond the cut-off value yields one point.
The highest possible score is six points.

In paper IV, we saw that patients referred to group C, whom all had RV failure (defined as an invasively measured right atrial pressure ≥10 mmHg), had a median RVF score of 4 points with an IQR of 3–5. The total IQR for groups A plus B was 0–2, with medians of 1 and 2 points, respectively.

App. 2. Conversion table of vascular resistance units

Two different units for vascular resistance were used in the original papers:

- dyn × s/cm^5 — papers I–III
- Wood units (WU) — paper IV

The units are converted as: 1 WU = 80 (dyn × s/cm^5).

In clinical practice, especially PVR is commonly referred to using WU. Furthermore, in the published results, indexed values are presented in paper II and III (PVRI and SVRI), while non-indexed PVR and SVR are used in paper I and IV.

To ease comparison between the four papers' baseline data, a table is included below, showing the corresponding (non-indexed) PVR values presented in both units.

In paper I, the mean of C1–C2 is used as baseline, while in papers II–III, the mean of C5–C6 is used (Fig. 10, p. 23). For paper IV, baseline data from all three groups are presented.

Paper (baseline point)	**PVR**	
	dyn × s/cm^5	**WU**
Paper I (C1–C2)	177	2.2
Papers II–III (C5–C6)	188	2.4
Paper IV, group A	150	1.9
Paper IV, group B	145	1.8
Paper IV, group C	206	2.6